

1-1-2007

MLCK/actin Interaction in the Contracting A7r5 Cell and Vascular Smooth Muscle

Sean Eric Thatcher
seanthatcher@uky.edu

Follow this and additional works at: <http://mds.marshall.edu/etd>

 Part of the [Biological Phenomena, Cell Phenomena, and Immunity Commons](#), [Medical Cell Biology Commons](#), and the [Musculoskeletal, Neural, and Ocular Physiology Commons](#)

Recommended Citation

Thatcher, Sean Eric, "MLCK/actin Interaction in the Contracting A7r5 Cell and Vascular Smooth Muscle" (2007). *Theses, Dissertations and Capstones*. Paper 162.

MLCK/actin Interaction in the Contracting A7r5 Cell and Vascular Smooth Muscle

by

Sean Eric Thatcher

Dissertation submitted to
the Graduate College
of
Marshall University
In partial fulfillment of the requirements
for the degree of

Doctor of Philosophy
In
Biomedical Sciences

Approved by

Michael Moore Ph.D
Larry Grover Ph.D
Elsa Mangiarua Ph.D
William McCumbee Ph.D
Gary Wright Ph.D, Committee Chairperson

Department of Pharmacology, Physiology, and Toxicology

Abstract

MLCK/actin Interaction in the Contracting A7r5 Cell and Vascular Smooth Muscle

By Sean Eric Thatcher

Myosin light chain kinase (MLCK) is an enzyme that phosphorylates the serine-19 residue on myosin regulatory light chains (MLCs) which serves to activate the Mg^{2+} -ATPase of myosin. This catalytic activity is thought to be the primary role of MLCK; however, it has recently been suggested that MLCK's actin binding and bundling properties may also be of importance in smooth muscle contraction. In the absence of calcium and calmodulin (CaM), MLCK will bundle actin filaments with its N-terminus. During calcium influx and subsequent CaM activation, MLCK binding to actin decreases resulting in unbundling of actin filaments and allows myosin and actin to slide past each other for force development. Despite these signals, some contractile agonists develop high levels of force in the relative absence of increased levels of intracellular calcium or MLC phosphorylation. One agonist that falls into this category is phorbol 12,13-dibutyrate (PDBu). PDBu activates the protein kinase C ($PKC\alpha$) pathway which inhibits myosin light chain phosphatase (MLCP) and allows the MLCs to stay in a phosphorylated state. $PKC\alpha$ can also phosphorylate the kinase domain of MLCK and inhibit activation via CaM. This pathway suggests that MLCK and its ability to bind to actin filaments may still be intact in PDBu-stimulated smooth muscle. Therefore, the present studies look at the interaction between MLCK and α - and β -actin, the two predominant isoforms found in vascular smooth muscle, during PDBu-induced contraction of A7r5 smooth muscle cells in culture and highly differentiated vascular smooth muscle freshly excised from the rat.

Acknowledgements

I wish to thank the Physiology and Anatomy Departments for giving me the foundation to study cardiovascular and smooth muscle physiology.

I also wish to thank my colleagues, Jason Black, Dawn Brown, Ava Dykes, Mike Fultz, and Chenwei Li for their helpful critiques and development of techniques that I used to study MLCK function.

I wish to thank my committee members Drs. Michael Moore, Larry Grover, Elsa Mangiarua, and William McCumbee for their help and guidance through my research here at Marshall University.

I would like to thank Drs. Akio Nakamura, Gao Ying, Hideyuki Tanaka, Takeshi Katayama, Sheng Li, Shinji Yoshiyama, and everyone that I met while in Maebashi, Japan. Special thanks to Dr. Kazuhiro Kohama for supporting and teaching me about MLCK and Japanese culture. I hope that our paths will meet again.

A special thanks to my mentor, Dr. Gary L. Wright, who allowed me to grow into a scientific researcher and supported me through the ups and downs of my research. I wish you the best and hope that you will continue to teach me about life in and out of biomedical research.

Table of Contents

Acceptance Page.....	i
Abstract.....	ii
Acknowledgments.....	iii
Table of Contents.....	iv
List of Figures.....	vi
List of Tables.....	viii
List of Symbols/Nomenclature.....	ix
Chapter One	
I. Dissertation Organization and Literature Review.....	1
II. Aspects of Muscle Contraction.....	2
Myosin.....	3
Actin.....	4
Cytoskeletal Remodeling.....	5
Podosomes.....	8
III. Kinase properties of MLCK.....	10
IV. Non-kinase properties of MLCK.....	13
V. FRET and Confocal Imaging.....	21
VI. Podosomes and Invadopodia.....	24
VII. Summary.....	28
VIII. References.....	30
Chapter Two	
MLCK/actin Interaction in the Contracting A7r5 Smooth Muscle Cell.....	38
Abstract.....	39
Introduction.....	40
Materials and Methods.....	42
Results.....	49
Discussion.....	53
References.....	57
Figure Legends, Figures, and Tables.....	60
Chapter Three	
MLCK/actin Interaction in Contracting Rat Aortic Tissue.....	72
Abstract.....	73
Introduction.....	74
Materials and Methods.....	76
Results.....	80

Discussion.....	83
References.....	86
Figure Legends, Figures, and Tables.....	88
Chapter Four	
Summary and Conclusions	
General Discussion.....	94
Future Work.....	97
Curriculum Vitae.....	98

List of Figures

Figure 1. MLC phosphorylation, intracellular calcium levels, degree of shortening, and isometric tension in vascular smooth muscle.....	7
Figure 2. Actin isoform distribution and remodeling in the A7r5 smooth muscle cell.....	8
Figure 3. Molecular anatomy of MLCK.....	16
Figure 4. Colocalization of MLCK and α -actin in untreated and PDBu (10^{-7} M)-stimulated A7r5 cells.....	66
Figure 5. Colocalization of MLCK and β -actin in untreated and PDBu (10^{-7} M)-stimulated A7r5 cells.....	66
Figure 6. Capture of donor emission before and after acceptor photobleaching in untreated and PDBu (10^{-7} M)-stimulated A7r5 cells (α -actin).....	67
Figure 7. Capture of donor emission before and after acceptor photobleaching in untreated and PDBu (10^{-7} M)-stimulated A7r5 cells (β -actin).....	67
Figure 8. Control experiments examining the responsiveness of the FRET system in different conditions of protein-protein association.....	68
Figure 9. Western blot analysis and bar graph of results from siRNA downregulation of MLCK in A7r5 cells.....	68
Figure 10. Immunolocalization of MLCK with α - or β -actin in nontargeting siRNA (negative control) and MLCK siRNA-transfected A7r5 cells under unstimulated conditions.....	69
Figure 11. Immunolocalization of MLCK with α - or β -actin in nontargeting siRNA (negative control) and MLCK siRNA-transfected A7r5 cells under PDBu (10^{-7} M)-stimulated conditions.....	69
Figure 12. Peptide-induced uptake of 1-25, 26-41, and 1-41 peptides of the N-terminus of MLCK.....	70
Figure 13. Microinjection of A7r5 cells with 1-41 peptide and an Alexa 594 fluorescent tracer.....	70
Figure 14. Time lapse phase-contrast microscopy for negative control and MLCK-siRNA transfected A7r5 cells.....	71

Figure 15. (MLC-P) at the serine-19/20 site in A7r5 cell negative control and MLCK-siRNA treated groups.....	71
Figure 16. Immunohistochemical staining of rat aortae for α -/ β -actin, myosin, and cholera toxin subunit-B (CT-B) “before photobleaching of acceptor” and “after photobleaching of acceptor”.....	91
Figure 17. Triple staining of MLCK (green), α -actin (red), and nuclei (blue) in longitudinal cut of rat aorta from control (unstimulated) and 10 minutes after the exposure of PDBu (10^{-7} M).....	92
Figure 18. Increased magnification of rat aorta depicting a single cell.....	92
Figure 19. Immunoblots of MLCK co-immunoprecipitations probed for α - and β -actin.....	93
Figure 20. Proposed model for MLCK/actin interaction in vascular smooth muscle.....	96

List of Tables

Table 1. Protein phosphorylation effects on MLCK kinase domain.....	12
Table 2. Donor and acceptor pairs for FRET analysis.....	22
Table 3. FRET values for % increase in donor fluorescence following photobleaching of acceptor molecules.....	64
Table 4. Whole cell immunofluorescence pixel counts in negative control and MLCK-siRNA transfected A7r5 cells stained for MLCK.....	65
Table 5. The percent of cells forming podosomes in response to 10^{-7} M phorbol 12,13-dibutyrate in negative controls and MLCK-siRNA transfected A7r5 cells.....	65
Table 6. FRET analysis of MLCK/actin interaction in rat aorta.....	90
Table 7. Percent of MLCK and α -/ β -actin interaction in comparison to tissue lysate.....	90

List of Symbols/Nomenclature

A-band	anisotropic band
α -Actin	alpha-actin
ADP	adenosine diphosphate
Arp2/3	Actin-related protein complex 2/3
ATP	adenosine triphosphate
ATPase	enzyme which catalyzes ATP cleavage
β -Actin	beta-actin
C-terminus	carboxyl-terminus of protein
Ca^{2+}	calcium
$[\text{Ca}^{2+}]_i$	intracellular calcium
CaM	calmodulin
Cdc42	cyclin-dependent kinase 42kDa
CHO	Chinese Hamster Ovary (cell line)
CPI-17	C-kinase protein inhibitor-17 kDa
CNBr	cyanogen bromide
c-Src	cellular form of the gene encoding a protein tyrosine kinase
DMEM	Dulbecco's modified Eagle medium
DTT	dithiothreitol
ECM	extracellular matrix
EDTA	ethylenediaminetetraacetic acid
EGTA	ethylene glycol-bis(2-aminoethylether)- <i>N,N,N',N'</i> -tetraacetic acid
eNOS	endothelial nitric oxide synthetase
ERK 1/2	extracellular signal regulated kinase complex 1/2
F-actin	filamentous actin
FAK	focal adhesion kinase
FCS	fetal calf serum
FITC	fluorescein isothiocyanate
FRET	fluorescence resonance energy transfer
g	relative centrifugal force
γ -Actin	gamma actin
G-actin	globular actin
GSK-3	glycogen synthase kinase-3
HeLa	Henrietta Lacks (cervical cancer cell line)
I-band	isotropic band
Ig	immunoglobulin
K^+	potassium (monovalent cation)
K_{CaM}	equilibrium constant for calmodulin
KRP	kinase-related protein
MAPK	mitogen activated protein kinase
Mg^{2+}	magnesium (divalent cation form)
MHC	myosin heavy chain
MLC	myosin light chain
MLCK	myosin light chain kinase
MLCP	myosin light chain phosphatase

MMPs	matrix metalloproteinases
MOPS	4-Morpholinepropanesulfonic acid
mRNA	messenger ribonucleic acid
MTBD	microtubule binding domain
N-terminus	amino-terminus of protein
Na ⁺	sodium (monovalent cation form)
nm	nanometers
NTCB	2-nitro-5-thiocyanobenzoic acid
nts	nucleotides
p190RhoGAP	p-subunit 190 KDa Rho-GTPase activating protein
PBS	phosphate buffered saline
PBS-T	phosphate buffered saline with 0.5% Tween-20
PDBu	phorbol 12,13-dibutyrate
PKA	Protein kinase A
PKC α	Protein kinase C alpha
PKC δ	Protein kinase C delta
PMSF	phenylmethylsulfonyl fluoride
PtK2	<i>Potorous tridactylus</i> (kangaroo cells derived from kidney)
PVDF	polyvinylidene difluoride
ROS	reactive oxygen species
RNAi	ribonucleic acid interference
siRNA	small, interfering ribonucleic acid
SM-A	smooth muscle myosin isoform A
SM-B	smooth muscle myosin isoform B
SM-1	smooth muscle myosin isoform 1
SM-2	smooth muscle myosin isoform 2
SMCs	smooth muscle cells
SRF	serum response factor
TIMPs	tissue inhibitors of matrix metalloproteinases
TMR	tetramethylrhodamine
TRITC	tetramethylrhodamine isothiocyanate
WASP	Wiscott-Aldrich syndrome protein
Z-line	Zwischen (German for “between,” in muscle “between the I-bands”)

Chapter One

I. Dissertation Organization and Literature Review

This dissertation is divided into four chapters with the first chapter discussing organization and giving a brief overview on MLCK function and aspects of skeletal versus smooth muscle contraction. Topics on fluorescence resonance energy transfer (FRET) and confocal imaging will also be evaluated along with podosome structure in the A7r5 cell. Similarities and differences between podosomes and invadopodia, a structure found in cancerous cell models, will also be discussed.

The second chapter deals with the N-terminal region of MLCK in the A7r5 cell and its interaction with α - and β -actin. Techniques utilized in these studies were: FRET, ribonucleic acid interference (RNAi), microinjection of peptides, and time-lapse phase contrast microscopy.

The third chapter looks at MLCK interaction with α - and β -actin in rat aortae. Techniques applied in this chapter were: FRET, co-immunoprecipitations, and confocal imaging.

The final chapter summarizes the data collected and implications for its use in understanding current pathophysiological states in the cardiovascular system. Furthermore, a discussion on future experiments as well as the development of novel techniques in the arena of smooth muscle cell migration will be discussed.

II. Aspects of Muscle Contraction

Typically when evaluating smooth muscle biology, comparisons are made between it and skeletal muscle. Skeletal muscle forms a striated appearance due to the presence of sarcomeres, overlapping regions of two filamentous proteins, actin and myosin. Actin and myosin interact in the central portion of the skeletal muscle sarcomere and is referred to as the A-band. The outer portion of the sarcomere contains only actin filaments, referred to as the I-band, and this region shortens during contraction. These actin filaments then attach to a region at the end of the skeletal muscle sarcomere referred to as the Z-line. The Z-lines define a single sarcomere. Many sarcomeres make up a myofibril and many myofibrils make up a skeletal muscle fiber. This highly structured appearance has given insight into skeletal muscle contraction; however, smooth muscle does not have this same phenotype. Smooth muscle, as its name implies, has a smooth appearance with actin and myosin arranged in various spatial patterns which rearrange upon contraction. Moreover, actin and myosin may undergo a change in organization in the contracting cell that is referred to as remodeling. The nature and mechanism of remodeling is not fully understood, but it is thought to exist since smooth muscle has the ability to shorten up to 80% of its original length (skeletal muscle can only shorten up to 30%). Hence, remodeling during contraction requires a coordinated reshaping of the contractile apparatus and the cytoskeleton of smooth muscle cells (Small and Gimona, 1998). The contractile apparatus of smooth muscle contains muscle actin and myosin with other proteins required for contraction (e.g. MLCK, CaM). The cytoskeleton is composed of non-muscle actin, desmin and/or vinculin, filamin, alpha-actinin, as well as other proteins. It is thought that the contractile apparatus is responsible for force

development in smooth muscle, while the cytoskeleton is involved in transmission of force to adjacent cells as well as tension maintenance (North et al., 1994). The contractile apparatus in smooth muscle is similar to skeletal muscle in that actin and myosin must slide past each other for shortening of the cell and force development. Since smooth muscle has the ability to maintain tension for long periods of time at low energy costs, it is thought that smooth muscle myosin “latches” onto the actin filament in the ADP-dependent state. This hypothesis is referred to as the latch model of smooth muscle contraction (Murphy et al., 1987), but since then smooth muscle myosins have been found to come in a number of different subtypes.

Myosin

Myosin II is the primary isoform found in muscle and is expressed in cardiac, skeletal, and smooth muscle tissues. Smooth muscle myosin ATPase is slower than its skeletal muscle counterpart. This is due either to the time-dependent release of the inorganic phosphate or the ADP molecule itself (Karagiannis and Brozovich, 2003). Two different isoforms of myosin II, which display differences in amino acid composition in the loop 1 region of the myosin head, are found in smooth muscle. One isoform has a 7 amino acid insert that is 20 amino acids away from the myosin ATPase site (Karagiannis and Brozovich, 2003). This isoform is referred to as SM-B. The other isoform does not contain this insert and is called SM-A. SM-B and SM-A can exist in other types of myosin, such as non-muscle myosin and myosin V; however their function is the same, to affect the kinetics of ATP hydrolysis at the myosin active site. SM-B is known to have a higher V_{\max} than SM-A and knockouts of SM-B in smooth muscle indicate decreases in shortening velocity and increases in force generation (Babu et al., 2004). The Babu et al.

(2004) study also noted that calponin levels increased in SM-B knockouts, while caldesmon levels were reduced. It is unknown at this point if SM-A or SM-B interacts with only certain thin filament-associated proteins. Another variation that can occur with myosin is at the tail region. Myosin consists of a hexamer of proteins that includes two heavy chains with two pairs of light chains. The tail region of the carboxy terminus (C-terminal) of myosin induces heavy chain dimers (Rovner et al., 2002). C-terminal myosin isoforms can be formed through alternative splicing of the gene. If a 43 amino acid insert is present then it is called SM-1. SM-1 contains a serine site that can become phosphorylated by casein kinase II and is thought to effect filament assembly in some types of smooth muscle (Rovner et al., 2002). The other isoform does not contain this insert and is referred to as SM-2. SM-1 and SM-2 have been shown to not affect ATPase kinetics therefore their regulation in contraction is unclear (Trybus, 1996b). However, it has been shown that the tail region of these isoforms can affect packing and assembly of the myosin filaments which may provide a role in structural dynamics of smooth muscle (Rovner et al., 2002). Ratios of SM-1 and SM-2 can change under certain conditions, such as pregnancy. There are also differences in their composition in tissues and cultured cell lines. Typically, vascular smooth muscle cells have more SM-1 than SM-2 in culture conditions (Adelstein and Sellers, 1996).

Actin

Actin exists as a globular protein known as G-actin and through ATP hydrolysis can form filaments known as (filamentous) F-actin. This creates a filament with polar ends and polymerization of actin can be influenced by proteins, such as the Arp 2/3 complex (Lehman et al., 1996). For polymerization to occur, an ATP molecule and a

divalent cation (Mg^{2+}) must be present (Lehman et al., 1996). Actin has a number of different isoforms and can exist as either a contractile-type or cytoplasmic-type of actin. The contractile-type is alpha (α -) or gamma (γ -) actin in smooth muscle. α -Actin is found in vascular smooth muscle and γ -actin is expressed in intestinal, esophageal, and tracheal smooth muscle. γ -Actin differs from α -actin in its biochemical and mechanical properties. Cytoplasmic actins (β - and γ -) are expressed in all tissues and can function in muscle contraction and structural integrity of the cytoskeleton. Actin structure is highly conserved with 95% or more of the amino acid sequence identical among these isoforms (Chaponnier and Gabbiani, 2004). Smooth muscle α -actin and γ -actin differ by only four amino acid residues at positions 1,4,5, and 360; whereas the contractile actins differ from cytoplasmic actins in positions 1,2,3, and 9 (Chaponnier and Gabbiani, 2004). One question that remains unanswered is whether these minor variations in the N-terminus convey functional differences among the actin isoforms in smooth muscle.

Cytoskeletal Remodeling

Through the use of *in vitro* motility assays and purification of F-actin, it has been shown that smooth muscle myosin ATPase shows no difference in the presence of skeletal or smooth muscle F-actin (Trybus, 1996a). It is thought that differences in actin remodeling of muscle is attributed to actin-binding proteins and differences in abundance of these proteins. For example, smooth muscle myosin can be expressed at 20% of the level of skeletal muscle (Murphy et al., 1997). This creates actin:myosin ratios of 10-15:1 in smooth muscle. How or whether myosin interacts with all of the actin present in smooth muscle is a question that remains unanswered. There are a number of actin- and myosin-binding proteins thought to influence smooth muscle contractile dynamics.

Caldesmon, calponin, and MLCK all occur in smooth muscle and are thought to modulate smooth muscle contraction (Gimona and Small, 1996, Marston and Huber, 1996, Stull et al., 1996). Relevant to the present studies, MLCK, found at high concentration in smooth muscle, is expressed at high levels early in embryology for skeletal and cardiac muscle, but this enzyme is absent in the adult tissue (Birukov et al., 1998). The finding that this or other actin-binding proteins interact with specific isoforms of actin could be important in our understanding of smooth muscle contraction. α -Actin and β -actin have been found to function differently in the A7r5 smooth muscle cell (Battistella-Patterson et al., 1997, Fultz et al., 2000, Li et al., 2001b). α -Actin remodels into podosomes while β -actin remains in filament structure; it was proposed that β -actin filaments maintain tension in the cytoskeleton while reorganization of α -actin was responsible for generating tension in the cell. This form of actin remodeling was referred to as asynchronous activation/inactivation (Battistella-Patterson et al., 1997). Phorbol esters induce podosomes in A7r5 cells and cause a slow but robust contraction in vascular smooth muscle tissue. In comparison to the potassium depolarization (Ca^{2+} -induced), two phases of tension generation can be identified and have been referred to as the fast-phase and the slow-phase of contraction (Battistella-Patterson et al., 1997) (Figure 1). The initial stimulus is an influx of calcium from the sarcoplasmic reticulum, extracellular space, or both into the cytosol that then binds to the CaM molecule. For the potassium contraction, calcium levels rise approximately 10-fold, but this can be less with other contractile agonists (Kamm and Stull, 1985, Nakajima et al., 1993, Oishi et al., 1991). This signaling cascade results in MLCK activation and MLC phosphorylation (Figure 1).

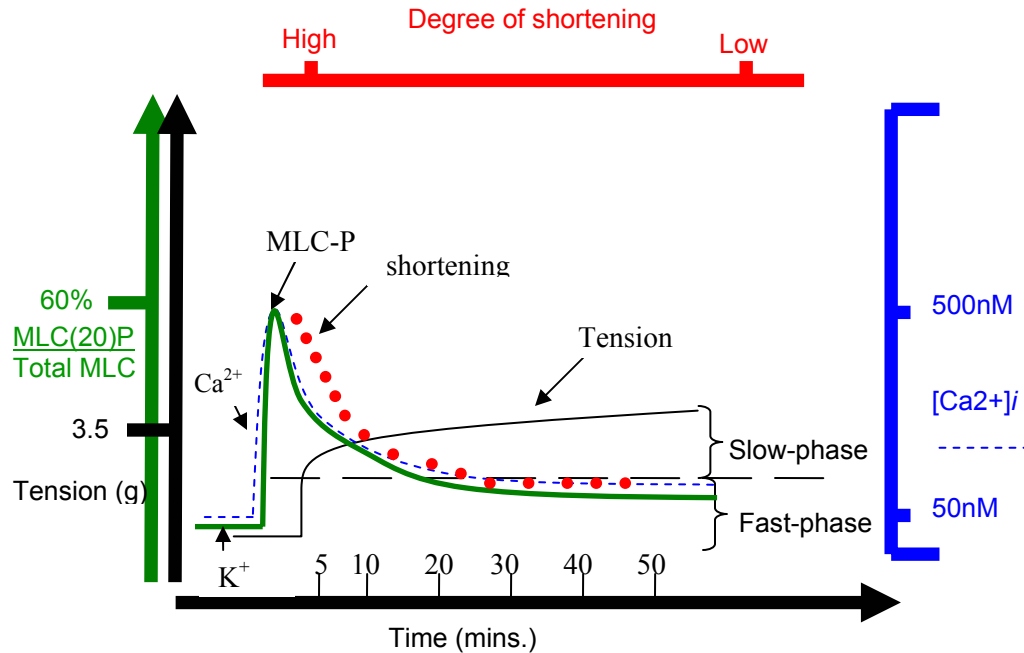


Figure 1. MLC phosphorylation, intracellular calcium levels, degree of shortening, and isometric tension in vascular smooth muscle. The contractile stimulus is 80 mM potassium. Green represents MLC, blue represents intracellular calcium, red represents degree of shortening, and black represents tension in grams. Taken from (Battistella-Patterson et al., 1997, Kamm and Stull, 1985)

Maximal levels of calcium result in a 60% rise in MLC phosphorylation that falls to baseline levels within the next 5-10 minutes (Kamm and Stull, 1985). After peak levels of calcium and MLC phosphorylation start to diminish, a fast-phase in tension generation occurs with a high degree of shortening (Figure 1). The fast-phase of contraction typically lasts for 5-10 minutes which correlates with the signals derived from intracellular calcium and MLC phosphorylation. However, smooth muscle tension will continue to rise slowly and reach a plateau phase (slow-phase of contraction) whereas the calcium levels will decrease along with MLC phosphorylation. The phorbol ester-induced contraction displays only the slow-phase of contraction and there is also limited calcium influx and MLC phosphorylation (Singer and Baker, 1987). In a study by Wright and Hurn (1994), cytochalasin D, a potent inhibitor of actin polymerization,

significantly decreased the slow-phase of the potassium contraction, however did not disrupt the fast-phase. In regards to phorbol esters, cytochalasin D also disrupted contraction (Wright and Hurn, 1994). These results suggest that actin polymerization is necessary for the slow-phase of smooth muscle contraction. This form of actin remodeling may explain why smooth muscle has a longer plateau in regards to the length-tension relationship in comparison to skeletal muscle. Furthermore, actin-binding proteins, such as MLCK, may influence this remodeling phenomenon.

Podosomes

The actin/myosin cytoskeleton of contracting A7r5 smooth muscle cells reorganizes into podosomes (Fultz and Wright, 2003). Podosomes are adhesive structures that are rich in actin and actin-binding proteins. These proteins are surrounded by a ring of myosin and create a column-like structure that is arranged in a rosette configuration within the cell (Figure 2).

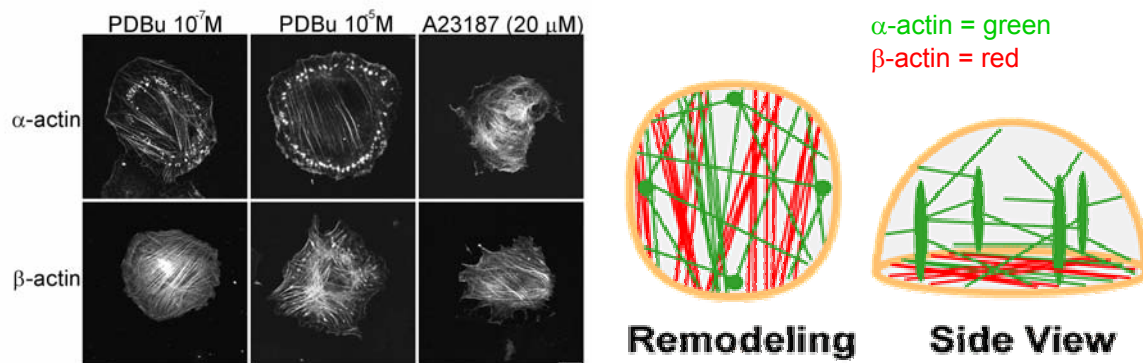


Figure 2. Actin isoform distribution and remodeling in the A7r5 smooth muscle cell. Note that the α -actin remodels into podosomes in a rosette fashion in the periphery of the cell. β -Actin stays in filaments after PDBu stimulation at 10^{-7} M concentration and remodels into podosomes at 10^{-5} M concentration. A23187 is a calcium ionophore that contracts A7r5 cells without forming podosomes.

Although it was earlier proposed that podosomes represent contractile structures in A7r5 cells, it has recently been suggested that these podosomes may be invasive structures subsequently referred to as invadopodia (Burgstaller and Gimona, 2005, Gimona and Buccione, 2006). Cells are most commonly grown on glass coverslips for imaging and this may not be an optimal condition for understanding smooth muscle cytoskeletal remodeling and contraction. Cells in the vasculature are surrounded by an extracellular matrix (ECM) and are arranged in an interconnected fashion with connecting gap junctions. In a study by Burgstaller and Gimona (2005), A7r5 cells were grown on fluorescently labeled fibronectin and podosomes were found to degrade this substrate. Matrix metalloproteinases (MMPs) are proteins responsible for degrading the extracellular matrix and MMPs are kept inactive through binding with tissue inhibitors of matrix metalloproteinases (TIMPs). Once this interaction is abolished, then MMPs can become activated and degrade the ECM. Smooth muscle cells contain MMP-2, -9, and -14 and these MMPs can degrade Type I, III, IV, V, VII, X, XI collagens, elastin, α -casein, gelatin, fibronectin, and other ECM proteins (Woessner and Nagase, 2000). It will be of interest to see if MMPs are located within the podosome and if inhibition of MMPs prevents the formation of podosomes (please refer to section VI for further evaluation). Whether or not podosomes represent focal adhesions or ECM degrading structures, podosomes contain the actin-myosin complex (Fultz and Wright, 2003) and show the presence of phosphorylated MLCs (Figure 15). The actin-myosin interaction and phosphorylation of MLCs are both necessary for smooth muscle contraction and migration.

An interesting difference between skeletal muscle and smooth muscle is that smooth muscle requires MLC phosphorylation in order to create force. The main site phosphorylated on MLC is a serine residue at position 19 of the protein. MLC phosphorylation typically increases within the first two minutes of exposure to the agonist and then precipitously starts to fall down to baseline levels (Figure 1). Despite this reduction in MLC phosphorylation, smooth muscle tension remains high. Explanations of how this occurs are still lacking at this time. Phorbol esters are responsible for activating PKC α and this initiates two signaling pathways. First, PKC α activates CPI-17 which inhibits myosin light chain phosphatase (MLCP) (Somlyo and Somlyo, 2003). This allows for the MLCs to remain in the phosphorylated state. Second, PKC may phosphorylate MLCs at serines 1,2 and threonine 9 (Stull et al., 1996). This causes an inhibition of MLCK phosphorylation of the light chains at serine 19. PKC α activation does not create a rise in MLC phosphorylation to the extent of potassium depolarization in swine carotid arteries (Singer, 1990). In uterine smooth muscle, oxytocin activates PKC with a resultant increase in contraction without an increase in RLC phosphorylation or $[Ca^{2+}]_i$ levels (Oishi et al., 1991). This phenomenon has been referred to as calcium sensitization because the contractile apparatus appears to be highly sensitive to small fluxes in calcium (Somlyo and Somlyo, 2003). Whether or not calcium sensitization, the latch hypothesis, or actin remodeling is the primary mechanism underlying smooth muscle contraction is still in question. Here we evaluate smooth muscle contraction in regards to MLCK activation in the phorbol ester-stimulated A7r5 cell and rat aortae.

III. Kinase properties of MLCK

MLCK can be classified as a multi-functional protein with a primary function to phosphorylate the serine-19 residue of the MLCs of myosin. The phosphorylation of MLCs activates the myosin ATPase which allows the power stroke to occur. In order for actin-myosin interaction to occur, the myosin binding site on actin must be available. Also, the distance between the two filamentous proteins must be exact in order for the appropriate sliding mechanism to be realized. If the filaments are too far away from each other there will be no interaction. Conversely, if the filaments are too close to one another, then tension generation is not optimal. MLCK-actin binding properties suggest an attractive coupling mechanism, because MLCK could regulate actin-myosin interaction through non-kinase properties not related to its kinase domain. It should be noted that caldesmon and calponin also regulate actin-myosin interaction, but neither protein has been characterized to have a kinase domain for phosphorylating the light chains of myosin.

MLCK can undergo autoregulation. The protein conformation of MLCK is such that a portion of the kinase is hidden by the autoregulatory segment located upstream from the kinase domain (pseudosubstrate region) (Stull et al., 1998). When activated, CaM binds to this region causing MLCK to undergo a conformational change, exposing the kinase domain and activating the enzyme. A plethora of protein kinases can phosphorylate portions of the kinase domain and C-terminal sequence of MLCK which increases the K_{CaM} (equilibrium constant of CaM) (Stull et al., 1997). This results in an increased requirement of activated CaM. Clusters of phosphoamino residues in the MLCK protein have been described and differences in the site of phosphorylation have been reported by different sources (Vorotnikov et al., 2002) (Table 1). Inhibition of

MLCK has been found in the $\text{Ca}^{2+}/\text{CaM}$ binding region (aa. 787-815) and has been called “site A.” The N-terminal region of the kinase-related protein (KRP) domain of MLCK has been called “site B” (~ aa. 828). Typically, site A phosphorylation can be blocked via binding of $\text{Ca}^{2+}/\text{CaM}$, however this is not absolute (Table 1).

Table 1. Protein phosphorylation effects on MLCK kinase domain (Vorotnikov et al., 2002)

Source of MLCK	Enzyme responsible for phosphorylating MLCK	Site A	Site B	Inhibition of phosphorylation through $\text{Ca}^{2+}/\text{CaM}$ binding
Avian	PKA	+	+	Site A
Sheep myometrium	PKA	+	+	Neither site
Bovine	PKG	-	+	Site B
Human platelet	PKG	- residue distinct from Site A	+	Site B
Human platelet	PKC	-	+	Site B
Endothelial cells	PAK			Ser-991, unique site on MLCK (does inhibit)

Site A phosphorylation inhibits the ability for MLCK to phosphorylate the MLC and thus prevents activation of the myosin ATPase. This form of regulation is thought to play a secondary role in the relaxation of smooth muscle. The primary mechanism is through expulsion of Ca^{2+} from the cytosol via $\text{Na}^+/\text{Ca}^{2+}$ exchangers and/or Ca^{2+} -ATPase pumps (Stull et al., 1997).

The effect of site B phosphorylation remains unclear as to function in smooth muscle. It is thought that site B phosphorylation may affect MLCK binding to myosin as well as cause the inhibition of myosin phosphorylation. MLCK also has the ability to phosphorylate itself (Kamm and Stull, 1985). MLCK’s autophosphorylation sites lie

within its kinase domain and in the N-terminal region of the protein. It is thought that autophosphorylation plays a role in MLCK activation; however, the *in vitro* data do not correlate well with *in vivo* data (Stull et al., 1996). In the future it will be of interest to understand how protein kinase phosphorylation of MLCK affects its catalytic activity in smooth muscle.

IV. Non-kinase properties of MLCK

In order to understand the non-kinase properties of MLCK, it is imperative to understand the techniques we and others have employed to study MLCK-actomyosin interactions. Typically, MLCK's tendency to degrade and its lower abundance than actin or myosin in smooth muscle make it a difficult protein to purify. Chicken or turkey gizzard supplies the most MLCK per gram of soft tissue and this still may only yield milligrams of intact MLCK (Adelstein and Klee, 1982). Actin and myosin are easier to purify although smooth muscle myosin ATPase activity can be reduced quite dramatically in the purification process (Adelstein and Sellers, 1996).

MLCK's ability to bind to actin was first demonstrated through centrifugation procedures (Hayakawa et al., 1999a). Actin, by itself, will not precipitate at low levels of centrifugation ($\leq 11,000$ g) and it is only after MLCK is added to the actin solution that a pellet will form after centrifugation. This is due to MLCK's ability to crosslink and bundle actin filaments (Kohama et al., 1996). As MLCK concentration increases, more actin bundles will form up to a saturated concentration (Hayakawa et al., 1999b). It has also been found that when Ca^{2+} /CaM is added to the solution, MLCK cannot bundle actin as effectively and more MLCK appears in the supernatant as opposed to the pellet when analyzed by gel electrophoresis (Hayakawa et al., 1994). MLCK appears to have two

types of actin-binding sites; one is a Ca^{2+} /CaM-sensitive site and the other is a Ca^{2+} /CaM-insensitive site. It is also interesting to note that MLCK has a higher binding affinity for purified myofilaments than to F-actin alone (Stull et al., 1998). This suggests that another protein contaminant may facilitate binding of MLCK on purified myofilaments that is absent on F-actin polymerized *de novo* (Stull et al., 1998).

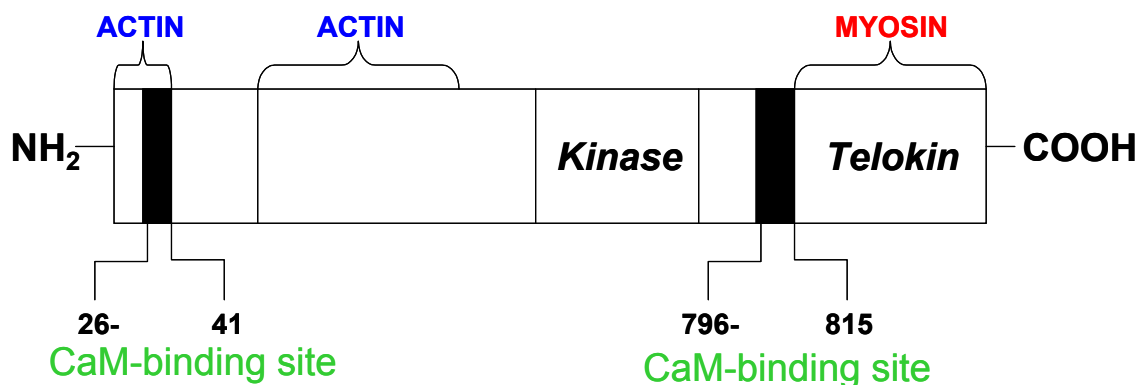
In order to understand where these sites are located in the MLCK protein, MLCK was subjected to cyanogen bromide (CNBr) which cleaves proteins at methionine (Met) residues and 2-nitro-5-thiocyanobenzoic acid (NTCB) which cleaves at cysteine residues (Gao et al., 2001). After cleavage, the CNBr created an aspartate (Asp)²-Met²¹³ fragment of MLCK that contained both Ca^{2+} /CaM-sensitive and -insensitive sites (Gao et al., 2001). NTCB created a fragment of Met¹-lysine(Lys)¹¹⁴ which was found to only contain the Ca^{2+} /CaM-sensitive site (Gao et al., 2001). The MLCK/actin-binding studies showed that the NTCB fragment was unable to bundle actin filaments and its binding activity was totally abolished by the Ca^{2+} /CaM complex. Because binding and bundling are two separate activities, the results further indicated at least two distinct binding sites. Bundling requires the presence of both Ca^{2+} /CaM-insensitive and -sensitive sites whereas binding requires the presence of only one actin-binding site. In this case, only the Ca^{2+} /CaM-insensitive site showed binding to actin filaments in the presence of the Ca^{2+} /CaM complex (Gao et al., 2001).

In order to get a more precise location of the actin binding sites, recombinant peptide fragments and site-directed mutagenesis were performed. Smith et al. (1999), reported that by deleting the first twenty-three amino acids of MLCK, 50% of the protein remained in the supernatant and did not bind to myofilaments. When they deleted the

first 39 or 58 amino acids from the N-terminal region, no significant binding occurred. This indicated that amino acid region 24-39 or 24-58 contained a significant actin binding structure (Smith et al., 1999). In a study by Ye et al. (1997), *E. coli* recombinant protein fragments were used to show that as the NN-fragment (aa. 1-526) concentration increased, more of the fragment was able to bind to actin (the NN-fragment contains both Ca^{2+} /CaM-sensitive and -insensitive sites). This binding was significantly affected when the Ca^{2+} /CaM-sensitive sites were deleted (NC-fragment). When the first 41 amino acids of the NN-fragment were deleted, a more significant decrease in actin-binding was seen in comparison to the NC-fragment. Also Ye et al. (1997) showed that the 1-41 peptide competitively inhibited the binding of the NN-fragment to actin. Therefore, it was concluded that the 1-41 amino acid sequence of MLCK contained the actin-binding core.

Once comparative sequence analysis was performed on the first seventy-five amino acids of MLCK, it was found that sequences were almost identical among various vertebrate species (Smith et al., 1999). To evaluate the key elements of this sequence, alanine substitutions were made at various points in the N-terminus of MLCK. Out of 10 substitutions that were made, peptides with alanines substituted at aspartate Asp-30 (D), phenylalanine (Phe)-31 (F), arginine (Arg)-32 (R), and leucine (Leu)-35 (L) showed decreased binding affinity for actin filaments. This sequence, called the DFRXXL motif, was found at 3 locations in the N-terminus of MLCK. One location is at residues 2-7, another is at 30-35, and the last motif is located at 58-63 (Smith et al., 1999). When D, F, and R were replaced with triple alanines, all three motifs were found to at least be partly involved in binding to actin. Residues 2-4 showed 47% of pellet left, 30-32 showed 57% of pellet left, and 58-60 showed 34% of pellet left (Smith et al., 1999).

Consequently, after identification of the actin-binding core, CaM-binding regions within the first 114 amino acids were studied by a process called surface plasmon resonance. Surface plasmon resonance is a process where a cuvette coated with CaM-dansyl has a fluorescence at 518 nm. Once a protein or Ca^{2+} ions binds to this compound, the intensity increases and the spectrum shifts to a shorter wavelength (470 nm). Treatment with MLCK and calcium in the presence of this CaM derivative caused a large, upward shift in fluorescence (Hayakawa et al., 1999b). Due to the fact MLCK contains two CaM-binding regions; one at the actin binding domain and one in its kinase domain, the N-terminus was further evaluated in the absence of the kinase domain. The fluorescent shift of the N-fragment and the 25/NN-fragment (1-25 aa. were missing) had a similar shift in fluorescence (Hayakawa et al., 1999b). The 41/NN-fragment did not bind to CaM and did not cause an upward shift in fluorescence (Hayakawa et al., 1999b). Upon synthesis of a 26-41 peptide and notation of an upward shift in fluorescence, it was concluded that this region contained the CaM-binding sensitive site (Figure 3).



•MDFRANLQRQ VKPKTLSEEE RKVHG (26) PQQVDFRSVLAKKGTP(41)

Figure 3. Molecular anatomy of MLCK. Redrawn from *Molecular Mechanisms of Smooth Muscle Contraction*, Chapter 2, Hayakawa et al., 1999b. Actin-binding regions are blue, the myosin-binding site is red, CaM-binding sites are green, and actin-binding amino acid residues are depicted in pink.

The C-terminal region of MLCK is also an area of intense research. The C-terminus of the MLCK gene has its own promoter within an intron of the DNA and can produce its own transcript forming a protein named KRP (kinase-related protein) or telokin (“telos” of the kinase). KRP weighs 17.7 kDa and was originally discovered as a by-product in the purification of calmodulin (Vorotnikov et al., 2002). KRP can bind to myosin keeping it in filamentous form (Shirinsky et al., 1993). This is thought to keep the contractile apparatus structured in resting cells. Although it keeps myosin structured, it does not affect MLC phosphorylation. In fact, KRP is noted for having a higher binding affinity for unphosphorylated myosin as opposed to the phosphorylated form (Stull et al., 1998). An interesting study by Gao et al. (2003) showed that a slightly larger fragment of the C-terminus of MLCK did play a role in enhancing the myosin ATPase activity without phosphorylation of the MLCs. Some groups suggest that KRP may be responsible for the dephosphorylation of myosin, since KRP applied to “chemically skinned” smooth muscle shows a relaxation effect (Krymsky et al., 2001). It is thought that this relaxation effect works via MLCP (Krymsky et al., 2001). Upon increases in KRP phosphorylation, MLCP activity will increase allowing MLC phosphorylation to decrease and contraction will subside. There are three identified sites in KRP that can become phosphorylated by protein kinases: serines 12, 15, 18 (Krymsky et al., 2001) (Serine 12 is the same as “site B” on the intact MLCK molecule). Protein kinases A/G can phosphorylate Ser 12, *in vitro*, while mitogen-activated protein kinase (MAPK) and glycogen synthase kinase-3 (GSK3) can phosphorylate Ser 18 and 15, respectively (Krymsky et al., 2001). It is also thought that the phosphorylation is ordered, that Ser 18 phosphorylation of MAPK will precede GSK3 phosphorylation of Ser 15. Despite the

complexity of KRP phosphorylation, one interesting fact is that phorbol esters (PDBu) will increase the level of KRP phosphorylation (Krymsky, et al., 2001). In the study by Krymsky et al. (2001), it was noted that KRP phosphorylation increases 25-40% of its resting value in carotid arteries. Although KRP levels go up, there is no change in the contractility of the tissue. It has been established that PKC can inhibit MLCP through CPI-17 (Somlyo and Somlyo, 2003). Whether or not KRP phosphorylation and PKC activation play additive roles with smooth muscle contraction remains a mystery.

Not only does MLCK have multiple functions, it has been shown that multiple isoforms exist for MLCK. One isoform, referred to as the long- or 220-kDa isoform of MLCK, is a protein expressed ubiquitously during embryonic development (Blue et al., 2002). It is identical to the short or 130-kDa isoform of MLCK, except that it has a long N-terminal extension of 955 amino acids (Gao et al., 2001). The 130-kDa isoform of MLCK is the adult form that is found in smooth muscle; however, even in adulthood the 220-kDa isoform is found in lung, kidney, liver, vas deferens, and bladder (Blue et al., 2002). In cell lines such as A10 or A7r5, both isoforms can be found (Poperechnaya et al., 2000). In nonmuscle cell lines, such as HeLa or PtK2, only the long isoform exists (Poperechnaya et al., 2000). Localization of the 130-kDa isoform is found in the perinuclear area with some stress fiber localization (Lin et al., 1999). The 220-kDa isoform however, is strictly located on the stress fiber and can be found in the cell cortex and cleavage furrow of dividing cells. Recently, it has been discovered that the 220-kDa isoform also has a microtubule-binding domain (MTBD) located in the N-terminal extension. This MTBD structure has lower affinity sites for actin in comparison to the DFRXXL motif and can influence the bundling, branching, and polymerization of tubulin

(Kudryashov et al., 2004). Actin and microtubules are important in mitosis and cell spreading and movement and it is thought that the 220-kDa isoform may be responsible for integrating the microtubule and actin filament networks (Kudryashov et al., 2004). The 220-kDa isoform of MLCK contains 2 additional DFRXXL motifs in comparison to the 130-kDa isoform. These additional DFRXXL motifs are thought to confer a higher affinity for actin than the smaller isoform of MLCK (Smith et al., 2002).

In the paper by Hatch et al. (2001), the first 147 amino acids of MLCK were sequenced and 3-D reconstructions on the actin filament were evaluated. From 3-D reconstructions, MLCK complexed with F-actin showed an increase in axial diameter compared to F-actin alone. When these data were fitted to molecular models of actin, it was found that MLCK attached to the C-terminal residues of subdomain-1 of one actin monomer and formed a bridge to the second actin monomer at residues 228-232, an alpha-helix in subdomain-4. One interesting note is that MLCK by itself is largely unstructured; however, when placed with F-actin it assumes a compact shape (Hatch et al., 2001). In comparison to other actin-binding proteins, such as calponin and caldesmon, MLCK binds to a unique position on the actin molecule (Hatch et al., 2001). This would be expected to prevent competition between MLCK and other proteins and allow MLCK to stably interact with actin. Neutron scattering data has been collected on the catalytic and autoinhibitory domains of skeletal MLCK complexed with CaM, MLC, and an ATP analog. In the presence of these protein partners, the centers of mass of CaM and MLCK come closer together. This compaction between CaM and MLCK is similar to the compaction between PKA and ATP binding (Stull et al., 1998). MLCK also contains fibronectin-like and three Ig-like structural motifs (Stull et al., 1998). These

motifs consist of about 100 amino acids and can be found in such proteins as titin and elastin (Stull et al., 1998). Stull et al. (1998) note that these motifs are typically found in elastic compounds and may provide resistance to passive tension development. It is thought that CaM binds to an area downstream of the catalytic domain, collapses, and moves down the autoregulatory segment to remove autoinhibition (Stull et al., 1998). Removal of the first 8 amino acid residues of CaM can reduce maximal activity of MLCK by 50%. Stull et al. (1998) further note that although activation of MLCK was changed, the binding affinities for these mutants were not different from the wild-type phenotype. Therefore, the N-terminus of CaM is important for activation but not for binding to the MLCK molecule. Not only can MLCK be found on the actin filament, but it has been localized to the nuclear matrix (Simmen et al., 1984). In chicken liver extracts, estrogen stimulation caused an increase in CaM and MLCK localization at the nuclear matrix (Simmen et al., 1984). MLCK has also been found in the nucleoli of PtK2 and CHO cell lines (Guerriero et al., 1981). In the N-terminus of mammalian MLCKs, a 12 residue repeat motif was found with an internal KP(A/V) sequence that may be responsible for chromatin binding (Gallagher et al., 1991). This KP(A/V) sequence has also been found in histone H1 and neurofilament proteins M and H (Gallagher et al., 1991). Neurofilament proteins are known to bind to single-stranded DNA.

The transcription of the MLCK gene is quite complex and recently some information on its regulation has come to light. The 220 and 130-kDa isoforms use the same promoter with an internal promoter located within exon 29 for KRP expression (Birukov et al., 1998). The promoter region of the MLCK gene contains a CAG box which allows serum response factor (SRF) to bind and increase expression of MLCK

(Han et al., 2006). It has been noted that the CAG box is found with other muscle specific genes, such as MHC, and that modulation of this promoter site could affect the contractile apparatus. In the spontaneously hypertensive rat (SHR) model, it has been shown that the CAG box has a string of 12 CT nucleotides (nts) that enhances the binding of SRF to the MLCK promoter (Han et al., 2006). Results from this study suggest that increased expression of MLCK causes a concomitant increase in blood pressure in the SHR rat. These results suggest that MLCK expression at the mRNA level initiates hypertension and could be a possible factor in idiopathic hypertensive cases in humans.

V. FRET and Confocal Imaging

Fluorescence Resonance Energy Transfer (FRET) is the nonradiative process of energy donation from one fluorophore to a nearby accepting fluorophore. Typically, FRET occurs at a spatial distance of 1-10 nanometers (nm) and is used to detect conformational changes of proteins (Kenworthy, 2001). Confocal microscopy is the process of using specific wavelengths of light to excite certain fluorophores and by using a pinhole aperture in front of the light detector, confocal rejects certain light diffraction and only accepts light that passes directly through the aperture. This improves spatial resolution by eliminating all out-of-focus light that is above and below the focal plane. Spatial resolution of most confocal microscopes is in the range of 200-500 nm and improvement on this resolution can be achieved through FRET protocols (Kenworthy, 2001). One protocol is a process called acceptor photobleaching. Acceptor photobleaching is the photodestruction of the acceptor fluorophore so that it can no longer accept energy from a nearby donor fluorophore.

In order for FRET to occur certain criteria must be met. One, the emission spectrum of the donor must overlap the excitation spectra of the acceptor. There are numerous donor and acceptor pairs and some of these are listed in Table 2.

Table 2. Donor and acceptor pairs for FRET analysis

Donor fluor	Acceptor fluor	Type of experiment (photobleaching, sensitized emission, etc.)	Reference
FITC	TRITC	Sensitized emission	(Dictenberg et al., 1998)
FITC	TMR	Acceptor photobleaching	(Chhabra and dos Remedios, 2005)
FITC	Rhodamine	Gradual acceptor photobleaching	(Kam et al., 1995)
Alexa488	Alexa555	Sensitized emission	(Chen et al., 2003)

Second, the dipoles of the fluorophores must be oriented parallel to one another. This is to insure energy transfer does not under- or overshoot the acceptor fluorophore. Finally, distance between the two fluorophores must be small in order for FRET to occur (1-10 nm). There are numerous indices one can use to measure FRET and one of the most common is transfer efficiency. Transfer efficiency is $E = 1 - (I_D / I_{DNA})$, where E represents transfer efficiency, I_D is the intensity of the donor in the presence of the acceptor and I_{DNA} is the intensity of the donor with no acceptor (Kenworthy, 2001). Forster distance is an index used to define the angstrom distance when energy transfer is 50%. In these studies, transfer efficiency or some deviation of this equation is used since the Forster distance requires some assumptions about the given system employed (e.g. dipole orientation).

FRET can be applied to various microscope setups. Wide-field microscopy is used to measure FRET and advantageous for multiple fluorophores using various excitation filters compared to conventional laser-scanning confocal microscopes. It has also been reported that charged-coupled cooled devices (CCDs) have greater sensitivities than photomultiplier tubes (PMTs) (Kenworthy, 2001). A disadvantage of wide-field

scopes is the long time needed in order to photobleach an acceptor fluorophore. Also, wide-field scopes do not provide targeted regions for photobleaching. Therefore, the entire viewing area must be photobleached. Confocal microscopes provide the ability to change the intensity of the laser power which allows for a reduction in photobleaching time constants. It can also target regions of interest inside of a cell or organelle that can be used to provide an internal control (Kenworthy, 2001). Typically, when photobleaching a region of interest, only that area will show a FRET effect while areas outside will show no response. In all cases, it is important to generate controls for evaluation of the FRET response. Positive controls may include evaluation of proteins that have a distance less than 10 nm. This is done by targeting a primary antibody with secondary antibodies that have both donor and acceptor fluorophores (Chen et al., 2003). In a similar vein, negative controls can be employed through the analysis of protein/protein interaction where no interaction should occur. This might be to label a membrane protein and a cytosolic protein when studying the interaction between two cytosolic proteins (Chen et al., 2003). There should also be single labeled specimens that have either donor-only or acceptor-only labels. This is used to confirm that signal bleedthrough or back bleedthrough does not occur in a given system (Chen et al., 2003). These controls will help define the type of interaction that is occurring with donor- and acceptor-labeled samples.

Recently, FRET has been employed to study the catalytic domain of MLCK (Isotani et al., 2004). CFP and YFP proteins were flanked on either side of the Ca^{2+} /CaM domain near the kinase site. FRET would be highest in the absence of CaM binding and lowest when the CaM binds to the regulatory region of MLCK. Isotani et al. (2004)

studied permeabilized smooth muscle bladder strips under KCl (high Ca^{2+} conditions) and carbachol (low Ca^{2+} conditions) situations. They found that MLCK exhibited an initial 20% increase in activation which then slowly declined. Carbachol caused a smaller increase in activation (~10%) which also declined with time. Despite the fact that calcium levels, MLC phosphorylation, and force were at maximal levels, MLCK was never fully activated. The authors conclude that this was due to limited amounts of CaM since CaM binds to other proteins (calponin and caldesmon) besides MLCK (Isotani et al., 2004). Together, the results suggest that a coordinated response between MLCK activation and inhibition of MLCP must be inherent in smooth muscle cells in view of such high levels of MLC phosphorylation and force development.

In summary, although MLCK is widely recognized as a central protein in smooth muscle contraction, the bulk of research interest has focused on its kinase properties. The present studies are focused on the N-terminal region of MLCK and its interaction with myosin and actin isoforms as they may contribute to force development. Here we examined this interaction in the A7r5 smooth muscle cell line and rat aorta using FRET analysis and confocal microscopy.

VI. Podosomes and Invadopodia

It has been recently discovered that smooth muscle cells also contain actin rich structures referred to as podosomes (Brandt et al., 2002, Burgstaller and Gimona, 2004, Fultz et al., 2000, Hai et al., 2002, Kaverina et al., 2003, Linder and Aepfelbacher, 2003, Linder and Kopp, 2005). Podosomes contain a number of actin-binding proteins and can be activated by the protein kinase C ($\text{PKC}\alpha$) signaling system in smooth muscle (Hai et al., 2002). The A7r5 cell line, an embryonic thoracic aorta cell, expresses many of the

smooth muscle markers found in differentiated smooth muscle (Firulli et al., 1998) and is recognized as a good model for the study of vascular smooth muscle. The A7r5 cell uses a PKC α signal that activates c-Src, a non-receptor tyrosine kinase (Brandt et al., 2002). Activation of c-Src then increases the activity of p190RhoGAP, a GTPase protein, that will result in decreased activity of RhoA (Brandt et al., 2002). These signaling schemes indicate that both serine/threonine phosphorylation via PKC α or MLCK and tyrosine phosphorylation via c-Src and focal adhesion kinase (FAK) are important for cell contraction with podosome initiation and development. Interestingly, endothelial cells require PKC α , PKC δ , and cyclin-dependent kinase-42 (cdc42) to initiate podosome development (Moreau et al., 2006, Tatin et al., 2006, Varon et al., 2006a, Varon et al., 2006b).

Structurally, podosomes are columns of actin surrounded by a ring of myosin and vinculin (Fultz and Wright, 2003). They protrude into the cytosol and cause an upward membrane invagination that contains the β_1 integrin family of proteins (Linder and Aepfelbacher, 2003, Linder and Kopp, 2005). Cancer cells contain similar structures that are used in cell migration and are referred to as invadopodia (Bowden et al., 1999, Bowden et al., 2001, Bowden et al., 2006, Mueller and Chen, 1991, Mueller et al., 1992). Invadopodia also require tyrosine phosphorylation, p190RhoGAP activation, and are filled with actin surrounded by a myosin ring. According to Artym et al., one difference between invadopodia and podosomes is that invadopodia do not contain a ring of vinculin (2006). Some other differences between invadopodia and podosomes are that podosomes are dynamic, forming in 2-10 minutes and then undergoing disassembly (Gimona and Buccione, 2006). Invadopodia typically form and last for 2-12 hours. Invadopodia also

form in juxtaposition to the Golgi apparatus whereas podosomes do not (Gimona and Buccione, 2006). Podosome configuration is significantly different between cell types. For example, osteoclasts and macrophages form podosomes throughout the cell body whereas smooth muscle podosomes form in the lamella close to adhesion spots (Linder and Aepfelbacher, 2003, Linder and Kopp, 2005). Typically, adhesion spots are found in the protruding lamellae away from recruitment of the Arp2/3 complex found associated with the podosome (Gimona and Buccione, 2006). In endothelial cells, podosomes form in a rosette pattern in the perinuclear region of the cell (Moreau et al., 2003). Both invadopodia and podosomes contain MMPs that degrade the extracellular matrix and allow for increased cell motility. There are 28 different MMP isoforms and certain cell types will express certain ones. In smooth muscle, MMP-2, -9, and MT1-MMP (membrane type 1, also known as MMP-14) are found to degrade the ECM. MMP-14 is confined to the membrane and MMP-2 and -9 are cytosolic proteins. Differences in localization are probably due to a signaling cascade; for instance, MMP-14 is thought to activate MMP-2 which then activates MMP-9 in smooth muscle (Woessner and Nagase, 2000). It is still uncertain how prominent a role the MMPs play in podosome formation since there are numerous other proteinases found in cells (e.g. lysosomal and endosomal). MMPs are kept in check by TIMPs and to date there are four known isoforms (TIMP1-4). Of these compounds, TIMP binding is MMP specific. TIMP-1 will bind to MMP-9 whereas TIMP-2 will bind to MMP-2 (Woessner and Nagase, 2000). MMPs require a zinc atom and cleavage of the propeptide sequence for activation. However, TIMPs can bind to both inactive and active forms of MMPs and this may indicate that MMPs are

needed for focal spots of degradation as opposed to a widely dispersed secretion of proteinases typically seen in the stomach and gastrointestinal tract.

MMP activation can occur through multiple pathways. One pathway is through formation of reactive oxygen species. Phorbol esters have been found to induce ROS in human and rabbit SMCs through activation of the PKC signaling system (Mietus-Snyder et al., 1997). This ROS accumulation occurs within the first 5 minutes of phorbol stimulation and increases transcription of the scavenger receptor found in smooth muscle. This receptor helps SMCs internalize oxidized lipoprotein and cause the development of foam cells. These receptors are found in macrophages as well and are thought to play a significant role in the development of atherosclerosis. Other types of ROS agonists include H₂O₂ and vanadate. Vanadate inhibits tyrosine phosphatases in cells resulting in increased levels of tyrosine phosphorylation (Mietus-Snyder et al., 1997). Whether or not phorbol esters initiate ROS accumulation in the A7r5 cell line is still not known at this time.

One way to study cell interaction with the substrate is through the development of collagen matrices in cell culture systems. At high collagen concentrations, collagen gels will solidify and provide a scaffold onto which cells can spread. This allows cells to become encased within an extracellular environment that is similar to smooth muscle cells *in vivo*. Cells will then remodel the collagen matrix and form focal adhesions (Song et al., 2000, Song et al., 2001). Recently, it has been suggested that SMCs send guidance and contact cues to other SMCs in order to develop interconnections. Netrin-1 is one of these cues that works through the ERK1/2-eNOS pathway via a feed-forward mechanism (Nguyen and Cai, 2006). Depending on the cell density used in developing collagen

matrices, experiments can be performed to study cell-matrix or cell-cell interactions and the signaling required for this interaction (Grinnell et al., 2003). In a study by Tamariz et al. (2002), low cell density (10^5 cells/mL) remodeled the collagen matrix differently than high cell density (10^6 cells/mL). The authors attribute this to the resistance developed within the collagen matrix and the formation of focal adhesions. Focal adhesions provide a link between the extracellular environment and the internal cytoskeleton of a cell. These focal adhesions then transmit tension generation to the cytoskeleton which results in the formation of actin stress fibers (Tamariz and Grinnell, 2002). High density gels are typically studied for matrix contraction and the Rho-kinase and MLCK signaling pathways are involved in contraction with bovine aortic smooth muscle cells (Song et al., 2003). The group also noted that calcium signals for cell contraction come from the intracellular cytosol as opposed to the extracellular space (Song et al., 2003). The authors noted that the actin polymerization machinery (WASP/cdc42) was involved in smooth muscle migration, but not matrix contraction. Our lab has noted that PDBu also induces matrix contraction in A7r5 cells, however calcium ionophores have not been studied to this point (unpublished observations). Collagen matrix contraction is the decrease in area occupied by both cells and collagen when a contractile stimulus has been given. Within a collagen matrix, PDBu-stimulated A7r5 cells do display podosomes, but these structures appear most abundantly in cells grown on glass coverslips (unpublished observations). A7r5 cell contraction and growth in collagen matrices will be of interest to those studying atherosclerosis and aortic aneurysm since SMC migration is a distinguishing characteristic of these disease phenotypes.

VII. Summary

The smooth muscle contraction has been defined as a slow and robust contraction with very little energy costs (Murphy and Rembold, 2005). The latch theory explains these given phenomenon as myosin latched to the actin in the ADP-dependent state with little ATP hydrolysis (Murphy et al., 1987). Latch, however, cannot explain the high degree of shortening evident in smooth muscle. It also cannot explain the differences in force development and tension maintenance in smooth muscle with different contractile agonists (e.g. PDBu and K^+).

Actin remodeling through polymerization pathways helps to explain this high degree of shortening by either increasing or decreasing the amounts of F-actin needed by the SMC (Wright and Hurn, 1994). Furthermore, actin-binding proteins could help to explain differences seen in tension development curves. PDBu and potassium depolarization may signal MLCK, calponin, or caldesmon to interact strongly or weakly with the actomyosin complex. In these experiments, the N-terminus of MLCK and interaction with actin was evaluated to better understand the actin-remodeling process. While no singular theory may explain smooth muscle contraction, we hope that these studies shed more light on actin remodeling and how the MLCK non-kinase domain is important in the A7r5 cell and vascular smooth muscle.

References

- Adelstein, R. S. and C. B. Klee. 1982. Purification of smooth muscle myosin light-chain kinase. *Methods Enzymol.* **85 Pt B**(298-308).
- Adelstein, R. S. and J. R. Sellers. 1996. Myosin structure and function, Biochemistry of smooth muscle contraction. *Academic Press*. 1st edition, 3-19.
- Artym, V. V., Y. Zhang, F. Seillier-Moiseiwitsch, K. M. Yamada and S. C. Mueller. 2006. Dynamic interactions of cortactin and membrane type 1 matrix metalloproteinase at invadopodia: defining the stages of invadopodia formation and function. *Cancer Res.* **66**(6): 3034-43.
- Babu, G. J., G. J. Pyne, Y. Zhou, C. Okwuchukuasanya, J. E. Brayden, G. Osol, R. J. Paul, R. B. Low and M. Periasamy. 2004. Isoform switching from SM-B to SM-A myosin results in decreased contractility and altered expression of thin filament regulatory proteins. *Am J Physiol Cell Physiol.* **287**(3): C723-9.
- Battistella-Patterson, A. S., S. Wang and G. L. Wright. 1997. Effect of disruption of the cytoskeleton on smooth muscle contraction. *Can J Physiol Pharmacol.* **75**(12): 1287-99.
- Birukov, K. G., J. P. Schavocky, V. P. Shirinsky, M. V. Chibalina, L. J. Van Eldik and D. M. Watterson. 1998. Organization of the genetic locus for chicken myosin light chain kinase is complex: multiple proteins are encoded and exhibit differential expression and localization. *J Cell Biochem.* **70**(3): 402-13.
- Blue, E. K., Z. M. Goeckeler, Y. Jin, L. Hou, S. A. Dixon, B. P. Herring, R. B. Wysolmerski and P. J. Gallagher. 2002. 220- and 130-kDa MLCKs have distinct tissue distributions and intracellular localization patterns. *Am J Physiol Cell Physiol.* **282**(3): C451-60.
- Bowden, E. T., M. Barth, D. Thomas, R. I. Glazer and S. C. Mueller. 1999. An invasion-related complex of cortactin, paxillin and PKCmu associates with invadopodia at sites of extracellular matrix degradation. *Oncogene.* **18**(31): 4440-9.
- Bowden, E. T., P. J. Coopman and S. C. Mueller. 2001. Invadopodia: unique methods for measurement of extracellular matrix degradation in vitro. *Methods Cell Biol.* **63**(613-27).
- Bowden, E. T., E. Onikoyi, R. Slack, A. Myoui, T. Yoneda, K. M. Yamada and S. C. Mueller. 2006. Co-localization of cortactin and phosphotyrosine identifies active invadopodia in human breast cancer cells. *Exp Cell Res.* **312**(8): 1240-53.
- Brandt, D., M. Gimona, M. Hillmann, H. Haller and H. Mischak. 2002. Protein kinase C induces actin reorganization via a Src- and Rho-dependent pathway. *J Biol Chem.* **277**(23): 20903-10.

- Burgstaller, G. and M. Gimona. 2004. Actin cytoskeleton remodelling via local inhibition of contractility at discrete microdomains. *J Cell Sci.* **117**(Pt 2): 223-31.
- Burgstaller, G. and M. Gimona. 2005. Podosome-mediated matrix resorption and cell motility in vascular smooth muscle cells. *Am J Physiol Heart Circ Physiol.* **288**(6): H3001-5.
- Chaponnier, C. and G. Gabbiani. 2004. Pathological situations characterized by altered actin isoform expression. *J Pathol.* **204**(4): 386-95.
- Chen, Y., J. D. Mills and A. Periasamy. 2003. Protein localization in living cells and tissues using FRET and FLIM. *Differentiation.* **71**(9-10): 528-41.
- Chhabra, D. and C. G. dos Remedios. 2005. Cofilin, actin and their complex observed in vivo using fluorescence resonance energy transfer. *Biophys J.* **89**(3): 1902-8.
- Chrzanowska-Wodnicka, M. and K. Burridge. 1996. Rho-stimulated contractility drives the formation of stress fibers and focal adhesions. *J Cell Biol.* **133**(6): 1403-15.
- Dictenberg, J. B., W. Zimmerman, C. A. Sparks, A. Young, C. Vidair, Y. Zheng, W. Carrington, F. S. Fay and S. J. Doxsey. 1998. Pericentrin and gamma-tubulin form a protein complex and are organized into a novel lattice at the centrosome. *J Cell Biol.* **141**(1): 163-74.
- dos Remedios, C. G., M. Miki and J. A. Barden. 1987. Fluorescence resonance energy transfer measurements of distances in actin and myosin. A critical evaluation. *J Muscle Res Cell Motil.* **8**(2): 97-117.
- Firulli, A. B., D. Han, L. Kelly-Roloff, V. E. Koteliansky, S. M. Schwartz, E. N. Olson and J. M. Miano. 1998. A comparative molecular analysis of four rat smooth muscle cell lines. *In Vitro Cell Dev Biol Anim.* **34**(3): 217-26.
- Fultz, M. E., C. Li, W. Geng and G. L. Wright. 2000. Remodeling of the actin cytoskeleton in the contracting A7r5 smooth muscle cell. *J Muscle Res Cell Motil.* **21**(8): 775-87.
- Fultz, M. E. and G. L. Wright. 2003. Myosin remodelling in the contracting A7r5 smooth muscle cell. *Acta Physiol Scand.* **177**(2): 197-205.
- Gallagher, P. J., B. P. Herring, S. A. Griffin and J. T. Stull. 1991. Molecular characterization of a mammalian smooth muscle myosin light chain kinase. *J Biol Chem.* **266**(35): 23936-44.
- Gao, Y., K. Kawano, S. Yoshiyama, H. Kawamichi, X. Wang, A. Nakamura and K. Kohama. 2003. Myosin light chain kinase stimulates smooth muscle myosin ATPase activity by binding to the myosin heads without phosphorylating the myosin light chain. *Biochem Biophys Res Commun.* **305**(1): 16-21.

- Gao, Y., L. H. Ye, H. Kishi, T. Okagaki, K. Samizo, A. Nakamura and K. Kohama. 2001. Myosin light chain kinase as a multifunctional regulatory protein of smooth muscle contraction. *IUBMB Life*. **51**(6): 337-44.
- Gimona, M. and R. Buccione. 2006. Adhesions that mediate invasion. *Int J Biochem Cell Biol*. **38**(11): 1875-92.
- Gimona, M., I. Kaverina, G. P. Resch, E. Vignal and G. Burgstaller. 2003. Calponin repeats regulate actin filament stability and formation of podosomes in smooth muscle cells. *Mol Biol Cell*. **14**(6): 2482-91.
- Gimona, M. and J. V. Small. 1996. Calponin, Biochemistry of smooth muscle contraction. *Academic Press*. 1st edition, 91-101.
- Grinnell, F., C. H. Ho, E. Tamariz, D. J. Lee and G. Skuta. 2003. Dendritic fibroblasts in three-dimensional collagen matrices. *Mol Biol Cell*. **14**(2): 384-95.
- Guerriero, V., Jr., D. R. Rowley and A. R. Means. 1981. Production and characterization of an antibody to myosin light chain kinase and intracellular localization of the enzyme. *Cell*. **27**(3 Pt 2): 449-58.
- Hai, C. M., P. Hahne, E. O. Harrington and M. Gimona. 2002. Conventional protein kinase C mediates phorbol-dibutyrate-induced cytoskeletal remodeling in a7r5 smooth muscle cells. *Exp Cell Res*. **280**(1): 64-74.
- Han, Y. J., W. Y. Hu, O. Chernaya, N. Antic, L. Gu, M. Gupta, M. Piano and P. de Lanerolle. 2006. Increased myosin light chain kinase expression in hypertension: Regulation by serum response factor via an insertion mutation in the promoter. *Mol Biol Cell*. **17**(9): 4039-50.
- Hatch, V., G. Zhi, L. Smith, J. T. Stull, R. Craig and W. Lehman. 2001. Myosin light chain kinase binding to a unique site on F-actin revealed by three-dimensional image reconstruction. *J Cell Biol*. **154**(3): 611-7.
- Hayakawa, K., H. Kishi, K. Kohama, Y. Lin, A. Nakamura, T. Okagaki, Y. Xue and L.-H. Ye. 1999a. Molecular mechanisms of smooth muscle contraction, Molecular Biology Intelligence Unit 5. *RG Landes Company*. 1st editon, 15-25.
- Hayakawa, K., T. Okagaki, L. H. Ye, K. Samizo, S. Higashi-Fujime, T. Takagi and K. Kohama. 1999b. Characterization of the myosin light chain kinase from smooth muscle as an actin-binding protein that assembles actin filaments in vitro. *Biochim Biophys Acta*. **1450**(1): 12-24.
- Isotani, E., G. Zhi, K. S. Lau, J. Huang, Y. Mizuno, A. Persechini, R. Geguchadze, K. E. Kamm and J. T. Stull. 2004. Real-time evaluation of myosin light chain kinase activation in smooth muscle tissues from a transgenic calmodulin-biosensor mouse. *Proc Natl Acad Sci U S A*. **101**(16): 6279-84.

- Ito, M., R. Dabrowska, V. Guerriero, Jr. and D. J. Hartshorne. 1989. Identification in turkey gizzard of an acidic protein related to the C-terminal portion of smooth muscle myosin light chain kinase. *J Biol Chem.* **264**(24): 13971-4.
- Kam, Z., T. Volberg and B. Geiger. 1995. Mapping of adherens junction components using microscopic resonance energy transfer imaging. *J Cell Sci.* **108 (Pt 3)**(1051-62).
- Kamm, K. E. and J. T. Stull. 1985. The function of myosin and myosin light chain kinase phosphorylation in smooth muscle. *Annu Rev Pharmacol Toxicol.* **25**(593-620).
- Karagiannis, P. and F. V. Brozovich. 2003. The kinetic properties of smooth muscle: how a little extra weight makes myosin faster. *J Muscle Res Cell Motil.* **24**(2-3): 157-63.
- Kaverina, I., T. E. Stradal and M. Gimona. 2003. Podosome formation in cultured A7r5 vascular smooth muscle cells requires Arp2/3-dependent de-novo actin polymerization at discrete microdomains. *J Cell Sci.* **116**(Pt 24): 4915-24.
- Kenworthy, A. K. 2001. Imaging protein-protein interactions using fluorescence resonance energy transfer microscopy. *Methods.* **24**(3): 289-96.
- Kishi, H., T. Mikawa, M. Seto, Y. Sasaki, T. Kanayasu-Toyoda, T. Yamaguchi, M. Imamura, M. Ito, H. Karaki, J. Bao, A. Nakamura, R. Ishikawa and K. Kohama. 2000. Stable transfectants of smooth muscle cell line lacking the expression of myosin light chain kinase and their characterization with respect to the actomyosin system. *J Biol Chem.* **275**(2): 1414-20.
- Kohama, K., T. Okagaki, K. Hayakawa, Y. Lin and R. Ishikawa. 1992. A novel regulatory effect of smooth muscle myosin light chain kinase on ATP-dependent actin-myosin interaction. *Jpn J Pharmacol.* **58 Suppl 2**(347P).
- Krymsky, M. A., D. S. Kudryashov, V. P. Shirinsky, T. J. Lukas, D. M. Watterson and A. V. Vorotnikov. 2001. Phosphorylation of kinase-related protein (telokin) in tonic and phasic smooth muscles. *J Muscle Res Cell Motil.* **22**(5): 425-37.
- Kudryashov, D. S., O. V. Stepanova, E. L. Vilitkevich, T. A. Nikonenko, E. S. Nadezhdina, N. A. Shanina, T. J. Lukas, L. J. Van Eldik, D. M. Watterson and V. P. Shirinsky. 2004. Myosin light chain kinase (210 kDa) is a potential cytoskeleton integrator through its unique N-terminal domain. *Exp Cell Res.* **298**(2): 407-17.
- Lehman, W., P. Vibert, R. Craig and M. Barany. 1996. Actin and the structure of smooth muscle thin filaments, Biochemistry of smooth muscle contraction. *Academic Press.* 1st edition, 47-58.
- Li, C., M. E. Fultz, W. Geng, S. Ohno, M. Norton and G. L. Wright. 2001a. Concentration-dependent phorbol stimulation of PKC α localization at the nucleus or subplasmalemma in A7r5 cells. *Pflugers Arch.* **443**(1): 38-47.

- Li, C., M. E. Fultz, J. Parkash, W. B. Rhoten and G. L. Wright. 2001b. Ca²⁺-dependent actin remodeling in the contracting A7r5 cell. *J Muscle Res Cell Motil.* **22**(6): 521-34.
- Lin, P., K. Luby-Phelps and J. T. Stull. 1997. Binding of myosin light chain kinase to cellular actin-myosin filaments. *J Biol Chem.* **272**(11): 7412-20.
- Lin, P., K. Luby-Phelps and J. T. Stull. 1999. Properties of filament-bound myosin light chain kinase. *J Biol Chem.* **274**(9): 5987-94.
- Linder, S. and M. Aepfelbacher. 2003. Podosomes: adhesion hot-spots of invasive cells. *Trends Cell Biol.* **13**(7): 376-85.
- Linder, S. and P. Kopp. 2005. Podosomes at a glance. *J Cell Sci.* **118**(Pt 10): 2079-82.
- Marston, S. B. and P. A. J. Huber. 1996. Caldesmon, Biochemistry of smooth muscle contraction. *Academic Press.* 1st edition, 77-88.
- Mietus-Snyder, M., A. Frieria, C. K. Glass and R. E. Pitas. 1997. Regulation of scavenger receptor expression in smooth muscle cells by protein kinase C: a role for oxidative stress. *Arterioscler Thromb Vasc Biol.* **17**(5): 969-78.
- Miura, M., T. Iwanaga, K. M. Ito, M. Seto, Y. Sasaki and K. Ito. 1997. The role of myosin light chain kinase-dependent phosphorylation of myosin light chain in phorbol ester-induced contraction of rabbit aorta. *Pflugers Arch.* **434**(6): 685-93.
- Moreau, V., F. Tatin, C. Varon, G. Anies, C. Savona-Baron and E. Genot. 2006. Cdc42-driven podosome formation in endothelial cells. *Eur J Cell Biol.* **85**(3-4): 319-25.
- Moreau, V., F. Tatin, C. Varon and E. Genot. 2003. Actin can reorganize into podosomes in aortic endothelial cells, a process controlled by Cdc42 and RhoA. *Mol Cell Biol.* **23**(19): 6809-22.
- Mueller, S. C. and W. T. Chen. 1991. Cellular invasion into matrix beads: localization of beta 1 integrins and fibronectin to the invadopodia. *J Cell Sci.* **99** (Pt 2)(213-25.
- Mueller, S. C., Y. Yeh and W. T. Chen. 1992. Tyrosine phosphorylation of membrane proteins mediates cellular invasion by transformed cells. *J Cell Biol.* **119**(5): 1309-25.
- Murphy, R. A., P. H. Ratz and C. M. Hai. 1987. Determinants of the latch state in vascular smooth muscle. *Prog Clin Biol Res.* **245**(411-3.
- Murphy, R. A., J. S. Walker and J. D. Strauss. 1997. Myosin isoforms and functional diversity in vertebrate smooth muscle. *Comp Biochem Physiol B Biochem Mol Biol.* **117**(1): 51-60.
- Murphy, R. A. and C. M. Rembold. 2005. The latch-bridge hypothesis of smooth muscle contraction. *Can J Physiol Pharmacol.* **83**(10): 857-64.

- Nguyen, A. and H. Cai. 2006. Netrin-1 induces angiogenesis via a DCC-dependent ERK1/2-eNOS feed-forward mechanism. *Proc Natl Acad Sci U S A.* **103**(17): 6530-5.
- North, A. J., M. Gimona, Z. Lando and J. V. Small. 1994. Actin isoform compartments in chicken gizzard smooth muscle cells. *J Cell Sci.* **107 (Pt 3)**(445-55).
- Oishi, K., H. Takano-Ohmuro, N. Minakawa-Matsuo, O. Suga, H. Karibe, K. Kohama and M. K. Uchida. 1991. Oxytocin contracts rat uterine smooth muscle in Ca²⁺(+)-free medium without any phosphorylation of myosin light chain. *Biochem Biophys Res Commun.* **176**(1): 122-8.
- Poperechnaya, A., O. Varlamova, P. J. Lin, J. T. Stull and A. R. Bresnick. 2000. Localization and activity of myosin light chain kinase isoforms during the cell cycle. *J Cell Biol.* **151**(3): 697-708.
- Rovner, A. S., P. M. Fagnant, S. Lowey and K. M. Trybus. 2002. The carboxyl-terminal isoforms of smooth muscle myosin heavy chain determine thick filament assembly properties. *J Cell Biol.* **156**(1): 113-23.
- Shirinsky, V. P., A. V. Vorotnikov, K. G. Birukov, A. K. Nanaev, M. Collinge, T. J. Lukas, J. R. Sellers and D. M. Watterson. 1993. A kinase-related protein stabilizes unphosphorylated smooth muscle myosin minifilaments in the presence of ATP. *J Biol Chem.* **268**(22): 16578-83.
- Simmen, R. C., B. S. Dunbar, V. Guerriero, J. G. Chafouleas, J. H. Clark and A. R. Means. 1984. Estrogen stimulates the transient association of calmodulin and myosin light chain kinase with the chicken liver nuclear matrix. *J Cell Biol.* **99**(2): 588-93.
- Singer, H. A. 1990. Phorbol ester-induced stress and myosin light chain phosphorylation in swine carotid medial smooth muscle. *J Pharmacol Exp Ther.* **252**(3): 1068-74.
- Small, J. V. and M. Gimona. 1998. The cytoskeleton of the vertebrate smooth muscle cell. *Acta Physiol Scand.* **164**(4): 341-8.
- Smith, L., M. Parizi-Robinson, M. S. Zhu, G. Zhi, R. Fukui, K. E. Kamm and J. T. Stull. 2002. Properties of long myosin light chain kinase binding to F-actin in vitro and in vivo. *J Biol Chem.* **277**(38): 35597-604.
- Smith, L., X. Su, P. Lin, G. Zhi and J. T. Stull. 1999. Identification of a novel actin binding motif in smooth muscle myosin light chain kinase. *J Biol Chem.* **274**(41): 29433-8.
- Somlyo, A. P. and A. V. Somlyo. 2003. Ca²⁺ sensitivity of smooth muscle and nonmuscle myosin II: modulated by G proteins, kinases, and myosin phosphatase. *Physiol Rev.* **83**(4): 1325-58.

- Song, J., B. E. Rolfe, I. P. Hayward, G. R. Campbell and J. H. Campbell. 2000. Effects of collagen gel configuration on behavior of vascular smooth muscle cells in vitro: association with vascular morphogenesis. *In Vitro Cell Dev Biol Anim.* **36**(9): 600-10.
- Song, J., B. E. Rolfe, I. P. Hayward, G. R. Campbell and J. H. Campbell. 2001. Reorganization of structural proteins in vascular smooth muscle cells grown in collagen gel and basement membrane matrices (Matrigel): a comparison with their in situ counterparts. *J Struct Biol.* **133**(1): 43-54.
- Song, L., J. J. Moon, H. Maio, G. Jin, P. C. Benjamin, Y. Suli, H. Yingli, U. Shunichi and S. Chien. 2003. Signal transduction in matrix contraction and the migration of vascular smooth muscle cells in three-dimensional matrix. *J. Vas. Res.* **40**(378-388).
- Stull, J. T., K. E. Kamm, J. K. Krueger, P. Lin, K. Luby-Phelps and G. Zhi. 1997. Ca²⁺/calmodulin-dependent myosin light-chain kinases. *Adv Second Messenger Phosphoprotein Res.* **31**(141-50).
- Stull, J. T., J. K. Krueger, K. E. Kamm, Z.-H. Gao, G. Zhi and R. Padre. 1996. Myosin light chain kinase, Biochemistry of smooth muscle contraction. *Academic Press.* 1st edition, 119-128.
- Stull, J. T., P. J. Lin, J. K. Krueger, J. Trehwella and G. Zhi. 1998. Myosin light chain kinase: functional domains and structural motifs. *Acta Physiol Scand.* **164**(4): 471-82.
- Tamariz, E. and F. Grinnell. 2002. Modulation of fibroblast morphology and adhesion during collagen matrix remodeling. *Mol Biol Cell.* **13**(11): 3915-29.
- Tatin, F., C. Varon, E. Genot and V. Moreau. 2006. A signalling cascade involving PKC, Src and Cdc42 regulates podosome assembly in cultured endothelial cells in response to phorbol ester. *J Cell Sci.* **119**(Pt 4): 769-81.
- Trybus, K. M. 1996. Myosin regulation and assembly, Biochemistry of smooth muscle contraction. *Academic Press.* 1st edition, 37-45.
- Varon, C., C. Basoni, E. Reuzeau, V. Moreau, I. J. Kramer and E. Genot. 2006a. TGFbeta1-induced aortic endothelial morphogenesis requires signaling by small GTPases Rac1 and RhoA. *Exp Cell Res.* **312**(18): 3604-19.
- Varon, C., F. Tatin, V. Moreau, E. Van Obberghen-Schilling, S. Fernandez-Sauze, E. Reuzeau, I. Kramer and E. Genot. 2006b. Transforming growth factor beta induces rosettes of podosomes in primary aortic endothelial cells. *Mol Cell Biol.* **26**(9): 3582-94.
- Vorotnikov, A. V., M. A. Krymsky and V. P. Shirinsky. 2002. Signal transduction and protein phosphorylation in smooth muscle contraction. *Biochemistry (Mosc).* **67**(12): 1309-28.

Woessner, J. F. and H. Nagase. 2000. Matrix metalloproteinases and TIMPs, Protein Profile. *Oxford Press*. 1-223.

Wright, G. and E. Hurn. 1994. Cytochalasin inhibition of slow tension increase in rat aortic rings. *Am J Physiol*. **267**(4 Pt 2): H1437-46.

Wright, G. L. and A. S. Battistella-Patterson. 1998. Involvement of the cytoskeleton in calcium-dependent stress relaxation of rat aortic smooth muscle. *J Muscle Res Cell Motil*. **19**(4): 405-14.

Ye, L. H., K. Hayakawa, H. Kishi, M. Imamura, A. Nakamura, T. Okagaki, T. Takagi, A. Iwata, T. Tanaka and K. Kohama. 1997. The structure and function of the actin-binding domain of myosin light chain kinase of smooth muscle. *J Biol Chem*. **272**(51): 32182-9.

Chapter Two

MLCK/Actin Interaction in the Contracting A7r5 Cell

Thatcher¹ SE, Fultz³ ME, Wright¹ C, Tanaka² H, Kohama² K, and Wright¹ GL.

¹Department of Pharmacology, Physiology, and Toxicology, The Joan C. Edwards School of Medicine, Marshall University, Huntington, WV 25704.

²Department of Molecular and Cellular Pharmacology, Gunma University, Maebashi, Japan

³Department of Biology, Morehead State University, Morehead, KY 40351.

Correspondence to:

Gary L. Wright
Professor of Pharmacology, Physiology, and Toxicology
The Joan C. Edwards School of Medicine
Marshall University
Huntington, WV 25704 USA
Phone: 304 696 7368
Fax: 304 696 7381
E-mail: wrightg@marshall.edu

Running title: MLCK/Actin interaction in contracting cells

Abstract

Previous work has suggested that in addition to its kinase activity, myosin light chain kinase exhibits non-kinase properties that could influence cytoskeletal organization. Colocalization imaging and fluorescence resonance energy transfer (FRET) analysis indicated α -actin/MLCK association in resting cells and in podosomes of phorbol 12,13-dibutyrate (PDBu)-stimulated A7r5 smooth muscle cells. By comparison, β -actin/MLCK association was observed in stress fibers and in diffuse distribution in the perinuclear region of both control and PDBu-treated cells. Downregulation of MLCK by siRNA transfection resulted in variable patterns of actin isoform reorganization in control cells. α -Actin formed a dense system of filaments at the cell periphery leaving the central region of the cells devoid of structure. In contrast, β -actin stress fibers disassembled with this isoform diffusely distributed in the cell. In PDBu-treated cells, transfection with MLCK-siRNA resulted in an approximate 70% reduction in the formation of podosomes. The introduction of a peptide containing the 1-41 N-terminal amino acid sequence of MLCK by peptide-mediated uptake or microinjection resulted in loss of α -actin stress fibers from the central region of the cell. The results indicate that MLCK plays an important role in maintaining α - and β -actin stress fibers and in the phorbol ester-induced reorganization of these isoforms. Furthermore, this role appears to be related to the N-terminal actin binding properties of the kinase.

Keywords: cytoskeleton, remodeling, podosomes, phorbol, FRET

Introduction

Myosin light chain kinase (MLCK) is a serine/threonine kinase important in the regulation of smooth muscle contraction (Kamm KE, 1985, Kamm and Stull, 1985). Two isoforms of MLCK have been identified (Bao et al., 2002, Poperechnaya et al., 2000) in cultured endothelial and smooth muscle cells. The larger 210 kDa isoform is thought to serve primarily in cytokinesis and cell division and interacts not only with actin but with microtubules as well (Kudryashov et al., 2004). Downregulation of the smaller 130 kDa isoform has suggested that this kinase is directly involved in smooth muscle contraction (Bao et al., 2002). In the presence of Ca^{2+} /calmodulin (CaM) complex, MLCK phosphorylates the serine-19 residue of the myosin regulatory light chains, activating myosin ATPase activity with subsequent force development (Kamm and Stull, 1985). In addition to its site of kinase activity located in the central region of the molecule, MLCK has multiple actin binding sites at its N-terminal (Kohama et al., 1992) and myosin binding activity at its C-terminal (Ito et al., 1989). Although research interest has centered on the kinase properties of MLCK, there is some evidence to suggest the enzyme is a multifunctional protein. For example, it is proposed that when myosin is fully phosphorylated MLCK exerts an inhibitory effect through its actin-binding domain and that MLCK binding of myosin could contribute to sustained force maintenance in smooth muscle (Gao et al., 2001).

Of particular interest is the in vitro observation that MLCK crosslinks actin filaments to form bundles and that this activity is abolished in the presence of Ca^{2+} /CaM complex (Hayakawa et al., 1999b). It has long been known that the N-terminus of MLCK is

necessary for binding to actin filaments (Lin et al., 1997, Smith et al., 1999).

Competitive binding studies have suggested MLCK contains two actin binding regions at residues 26-41 and 138-218 (Gao et al., 2001). In addition, Ca^{2+} /CaM binding sites have been identified at 26-41 and 787-815 residues (Ye et al., 1997). The 787-815 site regulates the kinase domain; whereas, the binding of Ca^{2+} /CaM at the 26-41 site inhibits actin binding and actin filament bundling. Taken together, these findings suggest the possibility of a mechanism for the simultaneous activation of myosin ATPase activity and the strategic release of crosslinked actin filaments for sliding filament force development. However, to our knowledge, the physiological role of MLCK in actin filament bundling has not been investigated.

In the present study, we utilized MLCK-siRNA and competitive binding of peptides containing the MLCK N-terminal actin binding site to evaluate the influence of MLCK on actin cytoskeletal structure in resting and contracted A7r5 smooth muscle cells. The results suggest that the actin binding properties of MLCK play an important role in determining actin cytoskeletal organization.

Materials & Methods

Chemicals. Unless otherwise stated all reagents were purchased from Sigma (St. Louis, MO).

Cell Culture. A7r5 cells are derived from embryonic rat thoracic aorta and were purchased from ATCC (Manassas, VA). Cells were plated on 75 cm² flasks and grown to approximately 85% confluence at 37°C in a humidified atmosphere of 5% CO₂ in air. The cells were maintained in Dulbecco's modified Eagles medium (DMEM) (Invitrogen, Carlsbad, CA) supplemented with 10% fetal bovine serum, 100 U/mL penicillin G, and 100 µg/mL streptomycin. Medium was changed every other day and cells were passaged at least once a week. Passaging was accomplished by addition of a trypsin/EDTA solution (Invitrogen, Carlsbad, CA) in phosphate-buffered saline (PBS) and collection of cells by centrifugation.

Immunocytochemistry. A7r5 cells were seeded on ethanol-flamed 22 x 22 mm, thickness 1 coverslips (Fisher, Inc., Chicago, IL) and allowed to grow for 24-48 hours. Cells were stimulated with phorbol 12, 13-dibutyrate (PDBu, 10⁻⁷M) for a period of 30 minutes. After stimulation, cells were fixed and permeabilized with ice-cold acetone for a period of 1 minute. Cells were then washed 3 times with PBS/0.5% Tween-20 (PBS-T) pH 7.5, followed by incubation in blocking solution containing 5% nonfat dry milk in PBS for 1 hour. MLCK staining was accomplished by incubation of cells in a 1:100 dilution of monoclonal MLCK clone K36, overnight at 4°C. Subsequently, cells were rinsed 3 times in PBS-T followed by an Alexa 488 anti-mouse IgG secondary antibody (Molecular Probes, Eugene, OR) at a 1:100 dilution for 1 hour. After rinsing in PBS-T, cells were reblocked in 5% nonfat milk to prevent cross-talk between the two primary

antibodies and were then stained for actin by incubation with α -actin clone 1A4, or β -actin clone AC-15 for 1 hour. Cells were rinsed 3 times in PBS-T followed by an Alexa 568 anti-mouse IgG secondary antibody (Molecular Probes, Eugene, OR) at a 1:100 dilution for 1 hour. Finally, cells were rinsed 3 times in PBS-T and mounted in Gel Mount medium (Biomedica Inc, Foster City, CA).

Confocal/FRET Microscopy. Immunostained cells were mounted on a Nikon Diaphot microscope and confocal microscopy was performed with a BioRad Model 1024 scanning system equipped with a krypton/argon laser. For FRET analysis, MLCK was labeled with Alexa 488 and served as the donor component of the system. α -Actin and β -actin were labeled with Alexa 568 and served as the acceptor molecules. The donor molecule (MLCK) was directly excited and the resulting emission was obtained with a 522DF32 bandpass filter. However, a portion of the energy of emission was transferred to neighboring Alexa 568 fluorophore resulting in emission that was captured on a second channel with a HQ598/40 bandpass filter. Subsequently, the sample was excited at the 568 nm laser line at 100% power to photobleach the acceptor (α -actin, β -actin) molecule and a second image of the cell was acquired again at the 488 nm laser line with the multichannel set to obtain MLCK fluorescence (522DF32) and to verify the absence of acceptor label 568 emission (HQ598/40). An intensity profile was generated for each image (Image J Software, NIH) and the resulting plot was analyzed with Peakfit V4.11 software (SPSS Science, Richmond, CA) to obtain the area under the curve. The values were then used to calculate the increase in fluorescence intensity after photobleaching. Because resonance energy transfer can only occur if the donor and acceptor molecules

are sufficiently close to one another, the resulting values were analyzed in comparison of treated and control cells as an index of the association between MLCK and either α - or β -actin. To evaluate the responsiveness of the FRET system as presently employed, a series of control experiments were performed. As a positive control, cells were incubated with either α - or β -actin specific antibodies labeled with both donor and acceptor fluorophores. In these experiments it was expected that the increased availability of closely associated binding sites would result in a significant increase in the FRET effect compared to the MLCK/actin evaluations. As a negative control, FRET analysis was performed on the association of α - and β -actin with the α -subunit of the calcium receptor located in the plasma membrane. In this case, it was expected that the FRET effect would be negligible. In addition, FRET analysis of MLCK/actin was conducted in the absence of acceptor fluorophore or donor fluorophore to evaluate the effects of autofluorescence and signal bleedthrough on results.

Generation and transfection of siRNA. A total of four siRNAs were developed against the C-terminal region of MLCK based on DNA sequence data obtained from NCBI's database, accession XP-213611 and derived from EST data via gene prediction method (GNOMON) and using the Ambion Target Finder:

5'-AATGAATCCTGGACGAAGACACCTGTCTC-3' (Sense target 44)
 5'-AAACAGAAGCAGGTCCTAAGTCCTGTCTC-3' (Antisense target 44)
 5'-AAGTCAGTTTAGATCGTCGCGCCTGTCTC-3' (Sense target 28)
 5'-AAGCGCTGCTAGATTTGACTGCCTGTCTC-3' (Antisense target 28)
 5'-AATCTGAGATCGAAGAGACGTCCTGTCTC-3' (Sense target 20)
 5'-AATGCAGAGAAGCTAGAGTCTCCTGTCTC-3' (Antisense target 20)
 5'-AAATACATGGCAAGAAGGAAGCCTGTCTC-3' (Antisense target 9)
 5'-AAGAAGGAAGAACGGTACATACCTGTCTC-3' (Sense target 9)

Each sequence was subjected to a blast search to ensure specificity for MLCK. Subsequently, siRNAs were constructed using Silencer siRNA construction kits (Ambion, Austin, TX) and transfections were performed using Oligofectamine (Invitrogen, Carlsbad, CA). Transfection efficiency was evaluated by labeling siRNAs with Cy3 using the Silencer siRNA labeling kit (Ambion, Austin, TX) (data not shown). The concentration of each siRNA was determined using a NanoDrop ND-1000 spectrophotometer (Nanodrop, Wilmington, DE) at a 260 nm wavelength. The four siRNAs were then prepared as a cocktail containing equal concentrations of each inhibitor.

To evaluate the effects of the downregulation of MLCK on actin cytoskeletal structure, cells were seeded onto glass coverslips, placed in 6-well culture dishes and allowed 24 hours for attachment. Subsequently, 50 nM siRNA/oligofectamine in Opti-Mem I was added to each well for a 5 hour incubation. The samples were then rinsed three times and returned to the incubator for 24 hours prior to experimentation. Control cells for these experiments were transfected with RISC-Free siRNA #1 (negative control) (Dharmacon RNA technologies, Lafayette, CO).

Western Blots. A7r5 cells were seeded on 100 mm culture plates and allowed to grow to confluence. The cells were then transfected with MLCK-siRNA cocktail or nonsense-siRNA (negative control) or Lamin A/C siRNA (positive control) (Dharmacon RNA technologies, Lafayette, CO) and returned to the incubator for 24 hours. The samples were then trypsinized and the cells pelleted by centrifugation. The pellet was rinsed and

then suspended in lysis buffer (10 mM MOPS, 1% NP-40, 5 mM EDTA, 0.5 mM EGTA, 1 mM DTT, 50 mM MgCl₂, 300 mM NaCl, 1 mM PMSF, 50 µg/mL leupeptin, chymostatin, and pepstatin A) and sonicated for 10 seconds at a low setting. The sample was again centrifuged and the protein concentration of the supernatant determined by BCA analysis (Pierce, Rockford, IL). The sample was then run on 8% and 12% polyacrylamide gels. Gels were blotted on PVDF membranes and probed with MLCK (K36 clone), Lamin A/C (mab636 clone) (Affinity Bioreagents, Golden, CO) and GAPDH (6C5 clone) (Ambion, Austin, TX) antibodies. Blots were visualized by chemiluminescence with ECL reagents (Amersham Pharmacia Biotech, Piscataway, NJ) and scanned using an Epson 2580 photo scanner. Autoradiograms were analyzed by Image J software.

Effects of MLCK N-terminus peptides. In a final series of experiments, we examined the effects of peptides containing the N-terminal CaM-sensitive actin binding site of MLCK on actin cytoskeletal structure in unstimulated A7r5 cells. Peptides containing the 1-25 (NH₂-MDFRANLQRQVKPKTLSEEERKVHG-COOH), 26-41 (NH₂-PQQVDFRSVLAKKGTP-COOH), and 1-41 N-terminal amino acid sequence of MLCK were conjugated to a peptide (NH₂-CRQIKIWFQNRRMKWKK-COOH) derived from *Drosophila* antennapedia homeodomain protein and have been shown to facilitate cellular uptake of peptides (Chen et al., 2001). The conjugated peptides were dissolved in DMEM at a concentration of 2.0 mg/mL and added to cells for 30 minutes. The cells were then rinsed and fixed with ice cold acetone for immunostaining and imaging. In a second study, the MLCK peptides were introduced directly into the cell by

microinjection. Cells were injected with a Pneumatic Pico Pump (World Precision Instruments, Sarasota, FL) at a pressure setting of 5 and time constant of 2 seconds using glass pipets pulled with a Flaming Brown Micropipette Puller (Sutter Instruments Co., Novato, CA). Peptide was dissolved (25 mg/mL) in injection buffer (10 mM Alexa 594 fluor in 200 mM KCl) while control cells received buffer only. Following injection, cells were returned to the incubator for a two hour recovery period prior to fixation and staining.

Time lapse phase-contrast microscopy. A7r5 cells were seeded in 35 mm culture dishes and treated with MLCK-siRNA or RISC-free siRNA #1. Cells were rinsed and incubated with CO₂-Independent DMEM (Invitrogen) supplemented with 1X GlutaMax-I (Invitrogen), pen-strep, and 10% FCS. Culture dishes were placed in a DH-35 Culture Dish Heater attached to a TC-324B Heat Controller (Warner Instruments, Hamden CT) and incubated at 37°C. Cells were then treated with PDBu with contractions monitored every 10 minutes for a total time of 140 minutes. Phase-contrast images were obtained with a 10X objective and a Nikon D70 SLR camera attached to a Nikon microscope.

Myosin Light Chain Phosphorylation at Serine-19/20 Site. A7r5 cells were seeded on coverslips and placed in 6-well plates. Cells were stimulated with phorbol esters at a concentration of 10⁻⁷M for 30 minutes. Cells were fixed with 2% paraformaldehyde for 15 minutes and permeabilized with 0.1% Triton X-100 for 20 minutes. Fixed samples were then blocked in 5% nonfat milk and treated with a rabbit anti-phospho-MLC antibody against the serine-19/20 site for 1 hour at a dilution of 1:100 (Rockland,

Gilbertsville, PA). Alexa 488 rabbit anti-IgG was used as the secondary antibody at a dilution of 1:100 for a period of 1 hour. Cells were rinsed with PBS-T and mounted according to immunocytochemistry protocol.

Statistics. All experiments were performed in triplicate unless otherwise indicated.

Differences between treatment groups were evaluated by Students' t-tests and one-way ANOVA using Sigma Stat V.2.03 (SPSS Science Inc., San Rafael, CA). Differences were considered significant at $p < 0.05$. Results are presented as mean \pm SEM throughout the figures.

Results

Colocalization imaging of unstimulated cells indicated that α -actin was incorporated into a dense system of stress fibers spanning the cell with MLCK diffusely distributed throughout the cell body (Fig. 4). In PDBu-contracted cells there was a loss in α -actin stress fibers with translocation of both α -actin and MLCK to podosomes (intensely staining bodies located in the peripheral region of the cell). By comparison, β -actin was present in stress fibers in both control and PDBu-treated cells (Fig. 5). MLCK appeared to be strongly colocalized with β -actin in stress fibers as well as in a diffuse structure located in the perinuclear region of the cell. FRET analysis revealed a strong association of α -actin and MLCK in stress fibers of control cells that was not apparent in colocalization images and verified α -actin/MLCK association in podosomes (Fig. 6). Moreover, these results suggested that the α -actin/MLCK association increased significantly (87%) in PDBu-contracted cells (Table 3a). FRET analysis also verified β -actin/MLCK association in stress fibers and the perinuclear structure of control and PDBu-treated cells (Fig. 7). However, unlike the α -actin/MLCK complex, β -actin/MLCK association was unchanged between control and PDBu-contracted cells (Table 3a). To our knowledge, this is the first study to demonstrate MLCK association with α -actin at podosomes. Furthermore, the results suggest recruitment of α -actin/MLCK association during phorbol ester-mediated contraction of the cell.

As a part of these studies, a series of control experiments were conducted to evaluate the possibility that nonspecific effects or other artifact contributed to FRET results. The responsiveness of the system to increased availability of closely associated antibody

binding sites (positive control) was tested by incubating α - or β -actin specific antibodies (1:1 ratio) with donor and acceptor fluorophores (Fig 8A). As expected, the increase in donor molecule fluorescent intensity after photobleaching of the acceptor fluorophore was significantly greater in these actin/actin comparisons than obtained in actin/MLCK analyses (Table 3b). Similarly expected, FRET analysis of the association of α - and β -actin with the α -subunit of the calcium receptor located in the plasma membrane (negative control) showed no change in donor fluorescence after photobleaching of the acceptor fluorophore (Fig 8B, Table 3c). Finally, donor fluorophore labeling of MLCK in the absence of acceptor fluorophore or the labeling of actin isoforms in the absence of donor fluorophore yielded negligible changes in donor fluorescence following the photobleaching procedure (data not shown) indicating insignificant effects of autofluorescence and signal bleedthrough on the FRET system. The results suggest that FRET analysis, as presently employed, may provide a good indication of protein-protein interaction.

In a final series of experiments, we tested the hypothesis that MLCK contributed to cytoskeletal structural integrity through its actin binding properties. Western analysis indicated only the presence of the 130 kDa isoform of MLCK in A7r5 cells. Western analysis (Fig 9a,b) and evaluation by immunofluorescence (Fig 9c, Table 4) further indicated an average 40% and 55% downregulation of 130 kDa MLCK content, respectively, in cells treated with MLCK-siRNA. Immunofluorescence studies further suggested a wide range of fluorescence intensities among these cells with the majority of MLCK-siRNA-treated cells (72.1%) at <1000 pixel counts compared to 3.2% of negative

control cells (Table 4). Consequently, the actin cytoskeletal structure of MLCK-siRNA-treated cells at <1000 pixel counts was compared with negative control cells at a 1000-2000 pixel fluorescent intensity range.

Negative controls showed typical α - and β -actin stress fibers in unstimulated cells (Fig 10). By comparison, MLCK-siRNA treated cells exhibited a loss in stress fibers with cell rounding. Interestingly, the effect of MLCK downregulation was different on α -actin versus β -actin structure. α -Actin formed a dense system of fibers at the cell periphery with the cell center devoid of structure. In contrast, β -actin stress fibers were generally absent in MLCK-siRNA-treated cells with this isoform concentrated in a network formation in the perinuclear region of the cell. Stimulation of negative control cells with 10^{-7} M PDBu resulted in the translocation of α -actin ($50.2 \pm 5.3\%$ of cells) and β -actin ($23.8 \pm 2.6\%$ of cells) to podosomes (Table 5, Fig. 11). MLCK-siRNA treatment of cells resulted in an approximate 70% reduction in podosome formation. Despite PDBu addition, these cells remained similar in appearance to unstimulated cells with peripheral α -actin stress fibers and diffuse distribution of β -actin with the cell.

The introduction of peptides containing 1-41 but not the 1-25 N-terminal amino acid sequence of MLCK into the cell either by peptide-induced uptake (Fig. 12) or by microinjection (Fig. 13) resulted in a loss in α -actin stress fibers in the central region of the cell similar in appearance to that seen in cells treated with MLCK-siRNA.

The majority of control cells ($76.7 \pm 2.8\%$) responded to phorbol esters with robust constriction (Fig. 14). By comparison, only $26.6 \pm 6.3\%$ of MLCK-siRNA treated cells showed evidence of responsiveness to phorbol. Surprisingly, the levels of phosphorylated MLC were similar between control and siRNA-treated cells (Fig. 15).

Discussion

Earlier work has indicated that MLCK has at least two actin binding regions and may crosslink actin filaments to form bundles (Gao et al., 2001, Hayakawa et al., 1999b). In addition to actin and myosin binding, MLCK contains two Ca^{2+} /CaM binding sites, one of which serves to activate kinase activity while the other negatively regulates actin binding at the N-terminal 26-41 actin binding site. Moreover, there is evidence to suggest that the binding affinity of the two sites is similar and that the actin binding site could bind Ca^{2+} /CaM under physiological conditions (Hayakawa et al., 1999b). Based on these observations, we speculated that MLCK crosslinking of actin filaments could be important in contributing to the organization of actin components of the contractile apparatus in smooth muscle. In the present study, we investigated the effect of downregulation of MLCK and use of peptides to competitively inhibit actin binding at the 26-41 site on actin structure in resting and PDBu-contracted A7r5 smooth muscle cells. Because the phorbol-induced contraction occurs in the absence of elevation in $[\text{Ca}]_i$ in these cells (Nakajima et al., 1993), cells in both resting and stimulated conditions were expected to exhibit the influence of MLCK actin filament crosslinking activity.

Whole cell FRET analysis, as presently employed, has been used successfully to evaluate protein-protein interactions in A7r5 cells (Dykes et al., 2003). Because the donor/acceptor must be within 10 nm distance from each other for efficient energy transfer (dos Remedios et al., 1987, Kenworthy, 2001) this technique provides a measure of protein-protein distances compatible with molecular interaction. FRET analysis indicated dynamic changes in the α -actin/MLCK contractile protein during the course of

PDBu-induced contraction and provided clearer resolution of actin/MLCK associated structure compared to that obtained with colocalization imaging. As expected, the labeling of actin with both donor and acceptor fluorophores resulted in a significantly higher FRET index than obtained for actin/MLCK while analysis of the association of actin with the α -subunit of the calcium channel located in the plasma membrane showed no FRET effect. These results suggest that whole cell FRET analysis is responsive to changes in protein-protein associations and can be used as a tool for assessing these interactions in fixed samples.

Use of colocalization and FRET analysis indicated a significant association of MLCK with α - and β -actin in stress fibers of unstimulated A7r5 cells. This was particularly evident in FRET images which indicated significant quenching of the donor component (Fig. 6). As previously reported (Fultz et al., 2000), PDBu-induced contraction resulted in the reorganization of α -actin into podosomes; whereas, β -actin was retained in stress fibers. In these cells, MLCK was observed in association with α -actin in podosomes and β -actin in stress fibers. Most notably, FRET analysis indicated an approximate 87% increase in α -actin/MLCK complex while β -actin/MLCK association was unchanged in contracted cells (Table 3). Taken together, these results indicated significant levels of actin/MLCK interaction in specific structures and that recruitment of α -actin/MLCK interaction may be important in the PDBu-induced contraction and actin reorganization in A7r5 cells.

MLCK-siRNA downregulation of MLCK resulted in a highly reproducible and characteristic change in actin structure. Unstimulated cells showed a general dissolution of β -actin with the loss of α -actin stress fibers from the central region of the cell. Reductions in the cellular content of MLCK were also observed to severely restrict the formation of podosomes in PDBu-treated cells. These results suggest a stabilizing influence of MLCK on actin stress fibers in resting cells and that the kinase plays an important role in contractile remodeling of actin. While these findings are consistent with an effect of MLCK crosslinking activity, internal strain can result in stress fiber formation (Chrzanowska-Wodnicka and Burridge, 1996) and a loss in basal MLCK kinase activity could have also contributed to results in these experiments.

Peptides containing the 26-41 N-terminal sequence have been successfully utilized to competitively inhibit MLCK at its Ca^{2+} /CaM-sensitive actin binding site (Gao et al., 2001). In the presence of these peptides or Ca^{2+} /CaM, actin binding is inhibited leaving MLCK bound to actin filaments at a second, Ca^{2+} /CaM-insensitive site. Because the Ca^{2+} /CaM binding affinity is similar at the 26-41 actin binding site and the 787-815 kinase activation site, it is likely that actin binding at this site is inhibited concurrent with activation of ATPase activity. Hence, there is little reason to believe that disassociation of MLCK from actin at the Ca^{2+} /CaM site would negatively affect basal kinase activity. This taken together with immunofluorescence data, indicating that the phosphorylation levels of myosin light chain were not altered by the downregulation of MLCK, makes it unlikely that reductions in internal strain on stress fibers contributed significantly to the results. The introduction of the 1-41 N-terminal peptide either by peptide-induced uptake

or microinjection resulted in the loss of stress fibers from the central region of cells. In aggregate, the results indicate that MLCK crosslinking property may be an important determinant of actin contractile structure.

Growing evidence suggests that the ability to reorganize the contractile apparatus and supporting cytoskeleton plays a central role in determining the contractile properties of smooth muscle (Gunst et al., 1993, Shen et al., 1997, Wright and Hurn, 1994, Wright and Battistella-Patterson, 1998). However, the exact nature of this remodeling and the mechanisms regulating cytoskeletal reorganization in contracting smooth muscle are not certain. Early work indicated that blockade of actin polymerization depressed force development (Battistella-Patterson et al., 1997, Wright and Hurn, 1994) suggesting filament elongation or the generation of new filaments is an important aspect of contractile remodeling. The present results further suggest that actin filament crosslinking by MLCK may play an important role in stabilizing actin structure in the precontracted cell and could contribute to actin reorganization during calcium-independent contraction. Based on these new findings and our previous work, we speculate that during Ca^{2+} /CaM-induced activation of MLCK kinase activity there is a simultaneous release of cross-linked actin filaments. Hence, in addition to activation of ATPase activity, MLCK may serve to both maintain actin contractile structure in the resting cell and release filaments for movement by myosin and force development. In the absence of this crosslinking activity, the loss in actin organization in the resting cell inhibits cell contraction and contractile remodeling.

References

- Bao J, Oishi K, Yamada T, Liu L, Nakamura A, Uchida MK, and Kohama K. 2002. Role of the short isoform of myosin light chain kinase in the contraction of cultured smooth muscle cells as examined by its down-regulation. *PNAS* 99(14):9556-9561.
- Battistella-Patterson AS Wang S, and Wright GL. 1997. Effect of disruption of the cytoskeleton on smooth muscle contraction. *Can. J. Physiol. Pharmacol.* 75:1287-1299.
- Chen L, Wright LR, Che-Hong C, Oliver SF, Wender PA, and Mochly-Rosen D. 2001. Molecular transporters for peptides: delivery of a cardioprotective ϵ PKC agonist peptide into cells and intact ischemic heart using a transport system, R7. *Chem. & Bio.* 8:1123-1129.
- Chrzanowska-Wodnicka M and Burridge K. 1996. Rho-stimulated contractility drives the formation of stress fibers and focal adhesions. *J. Cell Bio.* 133(6):1403-1415.
- Dos Remedios CG, Miki M, and Barden J. 1987. Fluorescence resonance energy transfer of distances in actin and myosin. A critical evaluation. *J. Muscle Res. and Cell Motil.* 8:97-117.
- Dykes AC, Fultz ME, Norton M, and Wright GL. 2003. Microtubule-dependent PKC- α localization in A7r5 smooth muscle cells. *Am. J. Cell Physiol.* 285:C76-C87.
- Fultz ME, Li C, Geng W, and Wright GL. 2000. Remodeling of the actin cytoskeleton in the contracting A7r5 smooth muscle cell. *J. Muscle Res. and Cell Motil.* 21:775-787.
- Gao Y, Ye L, Kishi H, Okagaki T, Samizo K, Nakamura A, and Kohama K. 2001. Myosin light chain kinase as a multifunctional regulatory protein of smooth muscle contraction. *IUBMB Life* 51:337-344.
- Gunst S, Wu M, and Smith D. 1993. Contraction history modulates isotonic shortening velocity in smooth muscle. *Am. J. Physiol.* 265(34):C467-C476.
- Hayakawa K, Okagaki T, Ye L, Samizo K, Higashi-Fujime S, Takagi T, and Kohama K. 1999. Characterization of the myosin light chain kinase from smooth muscle as an actin-binding protein that assembles actin filaments in vitro. *Biochimica et Biophysica Acta* 1450:12-24.
- Ito M, Dabrowska R, Guerriero UV, and Hartshorne DJ. 1989. Identification in turkey gizzard of an acidic protein related to the C-terminal portion of smooth muscle myosin light chain kinase. *J. Biol. Chem.* 264:13971-13974.

- Kamm KE and Stull JT. 1985. The function of myosin and myosin light chain kinase phosphorylation in smooth muscle. *Ann. Rev. Pharmacol. Toxicol.* 25:593-620.
- Kenworthy A. 2001. Imaging protein-protein interactions using fluorescence resonance energy transfer microscopy. *Methods* 24:289-296.
- Kohama K, Okagaki T, Hayakawa K, Lin Y, Ishikawa R, Shimmen T, and Inoue A. 1992. A novel regulatory effect of myosin light chain kinase from smooth muscle on the ATP-dependent interaction between actin and myosin. *Biochem. Biophys. Res. Commun.* 184(3):1204-1211.
- Kudryashov DS, Stepanova OV, Viltkevich EL, Nikonenko TA, Nadezhdina ES, Shanina NA, Lukas TJ, Van Eldik LJ, Watterson DM, and Shirinsky VP. 2004. Myosin light chain kinase (210 kDa) is a potential cytoskeleton integrator through its unique N-terminal domain. *Exp. Cell Res.* 298(2):407-417.
- Mehta D and Gunst S. 1999. Actin polymerization stimulated by contractile activation regulates force development in canine tracheal smooth muscle. *J. Physiol.(London)* 519(3):829-840.
- Nakajima S, Fujimoto M, and Veda M. 1993. Spatial changes of $[Ca^{2+}]_i$ and contraction caused by phorbol esters in vascular smooth muscle cells. *Am. J. Physiol.* 265:C1138-C1145.
- Pei-ju L, Luby-Phelps K, and Stull JT. 1997. Binding of myosin light chain kinase to cellular actin-myosin filaments. *J. Biol. Chem.* 272(11):7412-7420.
- Poperechnaya A, Varlamova O, Lin P, Stull JT, and Bresnick AR. 2000. Localization and activity of myosin light chain kinase isoforms during the cell cycle. *J. Cell Bio.* 151(3):697-707.
- Shen X, Wu M, Tepper R, and Gunst S. 1997. Mechanisms for mechanical response of airway smooth muscle to length oscillation. *J. Appl. Physiol.* 83(3):731-738.
- Smith L, Su X, Lin P, Zhi G, and Stull JT. 1999. Identification of a novel actin binding motif in smooth muscle myosin light chain kinase. *J. Biol. Chem.* 274(41):29433-29438.
- Wright GL and Battistella-Patterson AS. 1998. Involvement of the cytoskeleton in calcium-dependent stress relaxation of rat aortic smooth muscle. *J. Muscle Res. and Cell Motil.* 19:405-414.
- Wright GL and Hurn E. 1994. Cytochalasin inhibition of slow tension increase in rat aortic rings. *Am. J. Physiol. (Heart Circ. Physiol.)* 36(2):H1437-H1446.

Ye L, Hayakawa K, Kishi H, Imamura M, Nakamura A, Okagaki T, Takagi T, Iwata A, Tanaka T, and Kohama K. 1997. The structure and function of the actin-binding domain of myosin light chain kinase of smooth muscle. *J. Biol. Chem.* 272(51):32182-32189.

Figure Legends

Figure 4. Colocalization of MLCK and α -actin in untreated and PDBu (10^{-7} M)-stimulated A7r5 cells. MLCK was visualized with a monoclonal anti-MLCK, clone K36. α -Actin was visualized with a monoclonal anti- α -actin, clone 1A4. Secondary antibodies were Alexa 488 IgG and Alexa 568 IgG, respectively. Yellow color indicates colocalization of the two proteins. The white bar represents 20 μ m.

Figure 5. Colocalization of MLCK and β -actin in untreated and PDBu (10^{-7} M)-stimulated A7r5 cells. MLCK was visualized with a monoclonal anti-MLCK, clone K36. β -Actin was visualized with a monoclonal anti- β -actin, clone AC-15. Secondary antibodies were Alexa 488 IgG and Alexa 568 IgG, respectively. Yellow color indicates colocalization of the two proteins. The white bar represents 20 μ m.

Figure 6. Capture of donor emission before and after acceptor photobleaching in untreated and PDBu (10^{-7} M)-stimulated A7r5 cells. α -Actin was the acceptor and MLCK was the donor. Note the appearance of fibers and increase in intensity of emission at podosomes after photobleaching indicating significant quenching of donor emission by the acceptor.

Figure 7. Capture of donor emission before and after acceptor photobleaching in untreated and PDBu (10^{-7} M)-stimulated A7r5 cells. β -Actin was the acceptor and MLCK was the donor. Note the appearance of fibers after photobleaching indicating significant quenching of donor emission by the acceptor.

Figure 8. Control experiments examining the responsiveness of the FRET system in different conditions of protein-protein association. A) Positive control, either α -actin (a) or β -actin (b) were stained with both Alexa 488 (donor) and 568 (acceptor) fluorophores. Images (488 nm) were captured before and after photobleaching and the difference in their emission intensities was obtained using Paint Shop Pro V.7.04. B) Negative control, α -actin (c) or β -actin (d) were labeled with Alexa 568 (acceptor) with the α -subunit of the calcium-sensing receptor was stained with Alexa 488 (donor). As expected, this combination produced no FRET effect.

Figure 9. a.) Western blot analysis and b) bar graph of results from siRNA downregulation of MLCK in A7r5 cells. Non-targeting siRNA and siRNA-Lamin A/C were employed as negative and positive controls, respectively. GAPDH was probed to normalize for differences in protein loading. The bar graph indicates the averages from four individual experiments. c) In addition to Western blot analysis, whole cell immunofluorescence was compared between negative controls and MLCK-siRNA treated cells as a measure of MLCK downregulation. Red indicates MLCK, whereas blue color indicates nuclei stained with TO-PRO-3 dye.

Figure 10. Immunolocalization of MLCK with α - or β -actin in nontargeting siRNA (negative control) and MLCK siRNA-transfected A7r5 cells under unstimulated conditions. MLCK was visualized with a monoclonal, anti-MLCK antibody (K36 clone) followed by an Alexa 568 IgG secondary antibody. α -Actin and β -actin were visualized with a monoclonal anti- α -actin (1A4 clone) and a monoclonal anti- β -actin (AC-15 clone)

followed by an Alexa 488 IgG secondary antibody. Confocal settings for the MLCK panel were kept constant for the different treatments. White bar represents 40 μm .

Figure 11. Immunolocalization of MLCK with α - or β -actin in nontargeting siRNA (negative control) and MLCK siRNA-transfected A7r5 cells under PDBu (10^{-7}M)-stimulated conditions. MLCK was visualized with a monoclonal, anti-MLCK antibody (K36 clone) followed by an Alexa 568 IgG secondary antibody. α -Actin and β -actin were visualized with a monoclonal anti- α -actin (1A4 clone) and a monoclonal anti- β -actin (AC-15 clone) followed by an Alexa 488 IgG secondary antibody. Confocal settings for the MLCK panel were kept constant for the different treatments. White bar represents 40 μm .

Figure 12. Peptide-induced uptake of 1-25, 26-41, and 1-41 peptides of the N-terminus of MLCK. Peptides were conjugated to a peptide derived from *Drosophila* Antennapedia homeodomain protein to facilitate uptake and incubated with cells for 30 minutes. An α -actin FITC antibody (clone 1A4) was used for visualization of actin filaments. In a, b) A7r5 cells incubated with 1-25 peptide. c, d) A7r5 cells incubated with 26-41 peptide. e, f) A7r5 cells incubated with 1-41 peptide.

Figure 13. Microinjection of A7r5 cells with 1-41 peptide and an Alexa 594 fluorescent tracer. Control cells were injected with Alexa 594 tracer in a 200 mM K^+ buffer solution while experimental cells included the 1-41 peptide. α -Actin staining was performed with

FITC-conjugated antibody (clone 1A4) and used for visualization of actin filaments.

White bar represents 20 μm .

Figure 14. Time lapse phase-contrast microscopy for negative control and MLCK-siRNA transfected A7r5 cells. Cells were treated with PDBu ($10^{-7}M$) and cell images were obtained every 10 minutes for a total time of 140 minutes.

Figure 15. a.) (MLC-P) at the serine-19/20 site in A7r5 cell negative control and MLCK-siRNA treated groups. Cells were treated with PDBu ($10^{-7} M$) for 30 minutes and imaged with identical confocal settings for all groups. Scale bar represents 20 μm . b.) Bar graph analysis of (MLC-P)/cell area for the various treatment groups. Significant differences between the negative control and the MLCK-siRNA groups are reported at $p<0.05$.

Table 3. FRET values for % increase in donor fluorescence following photobleaching of acceptor molecules.

<u>a. Actin/MLCK</u>	<u>% Increase in Fluorescence</u>
<u>Control Cells</u>	
α -actin (N=20)	13.2 \pm 1.3
β -actin (N=20)	14.9 \pm 1.4
<u>PDBu-treated Cells (10⁻⁷M)</u>	
α -actin (N=20)	24.7 \pm 1.8*
β -actin (N=20)	12.9 \pm 0.9
<u>b. Positive Control</u>	
α -actin (N=15)	82.5 \pm 3.1
β -actin (N=5)	43.9 \pm 4.1
<u>c. Negative Control</u>	
α -actin (N=10)	-1.5 \pm 5.2
β -actin (N=10)	-3.0 \pm 5.2

An asterisk indicates a significant difference between control versus PDBu-treated cells, $p < 0.05$. Values are means \pm SE. **Note:** a) Values indicating actin/MLCK association in control and PDBu-treated A7r5 cells. b) Positive control in which both donor and acceptor fluorophores were labeled to anti- α -actin or anti- β -actin antibodies. c) Negative control in which α -actin or β -actin interaction with a plasma membrane-bound calcium channel protein was evaluated.

Table 4. Whole cell immunofluorescence pixel counts in negative control and MLCK-siRNA transfected A7r5 cells stained for MLCK.

<u>a. Average Intensity</u>	<u>Pixel Count</u>	
Negative Control	1715 ± 62	
MLCK-siRNA	945 ± 65	

<u>b. Range of Values</u>	<u>% of Cells</u>	
<u>Pixel Counts</u>	<u>Negative Control</u>	<u>MLCK-siRNA</u>
>3000	5.7	1.0
>2000	21.3	7.2
>1000	69.7	19.5
>500	3.2	49.5
<500	0	22.6

Table 4a values are means ± SE.

Table 5. The percent of cells forming podosomes in response to 10^{-7} M phorbol 12,13-dibutyrate in negative controls and MLCK-siRNA transfected A7r5 cells.

<u>Treatment</u>	<u>α-Actin</u>	<u>β-Actin</u>
Negative Control	50.2 ± 5.3	23.8 ± 2.6†
MLCK-siRNA	15.3 ± 2.6*	7.9 ± 1.7*

An asterisk (*) or (†) indicates a significant difference between negative control versus MLCK-siRNA and α- versus β-actin, respectively, $p < 0.05$. **Note:** Cells were immunostained for either α-actin or β-actin. Values are means ± SE and represent the average from a minimum of 500 cells obtained in four independent experiments.

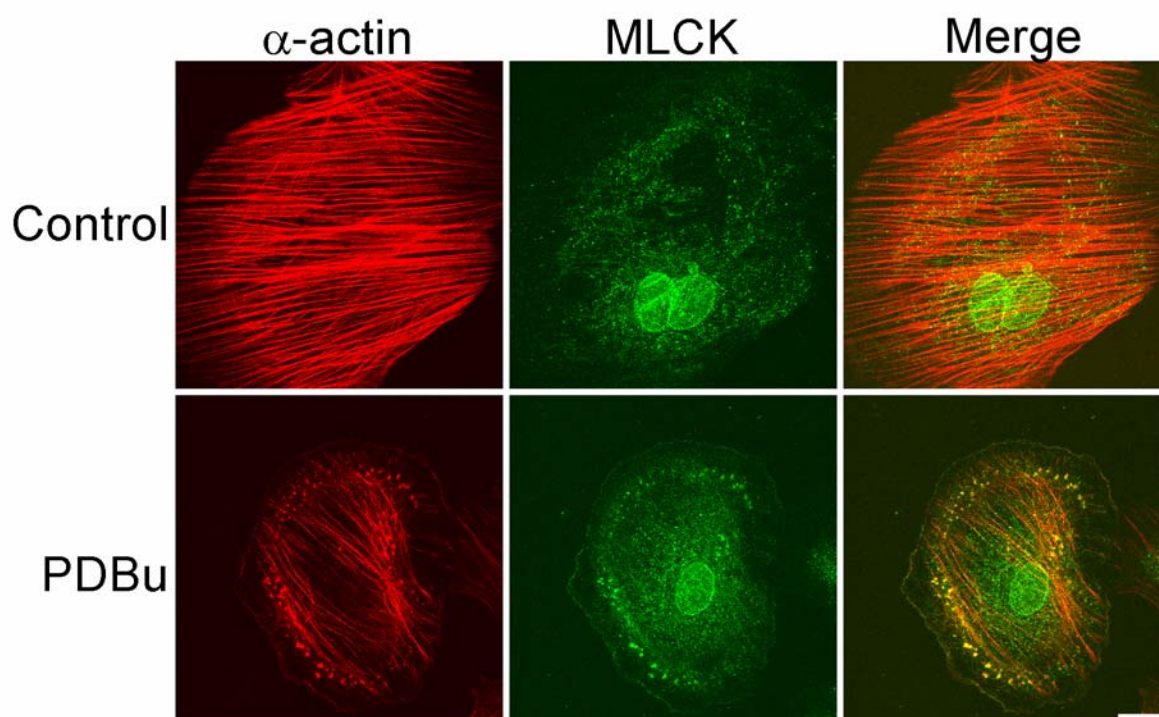


Figure 4.

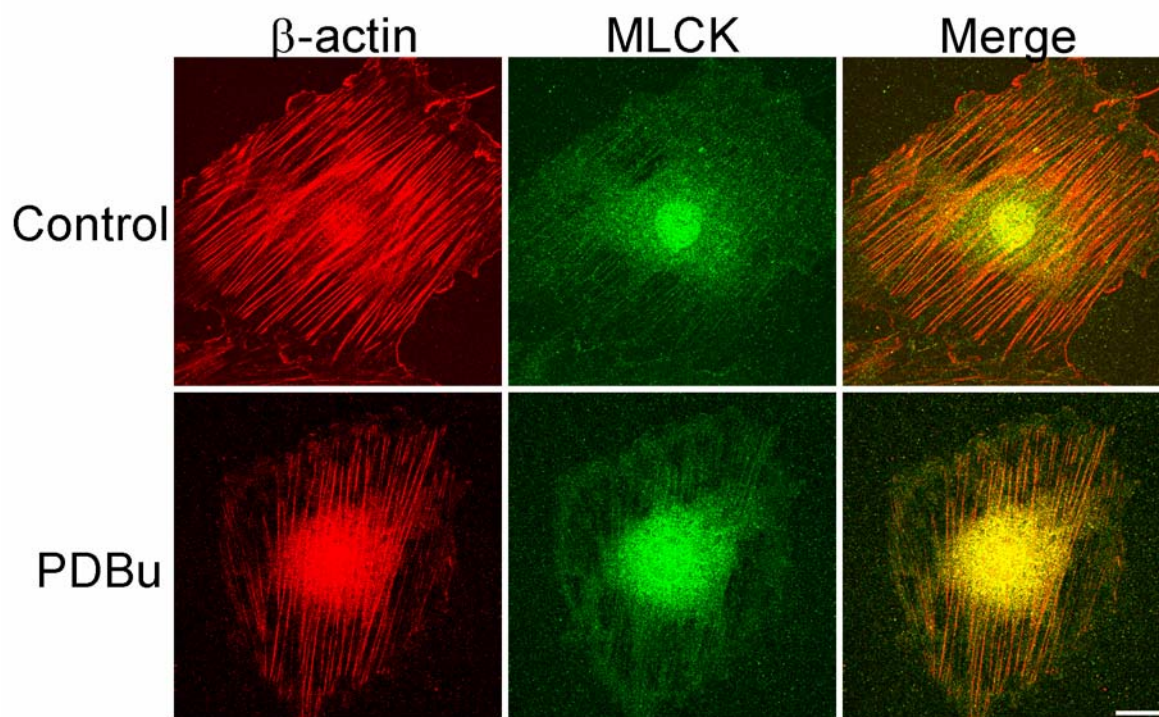


Figure 5.

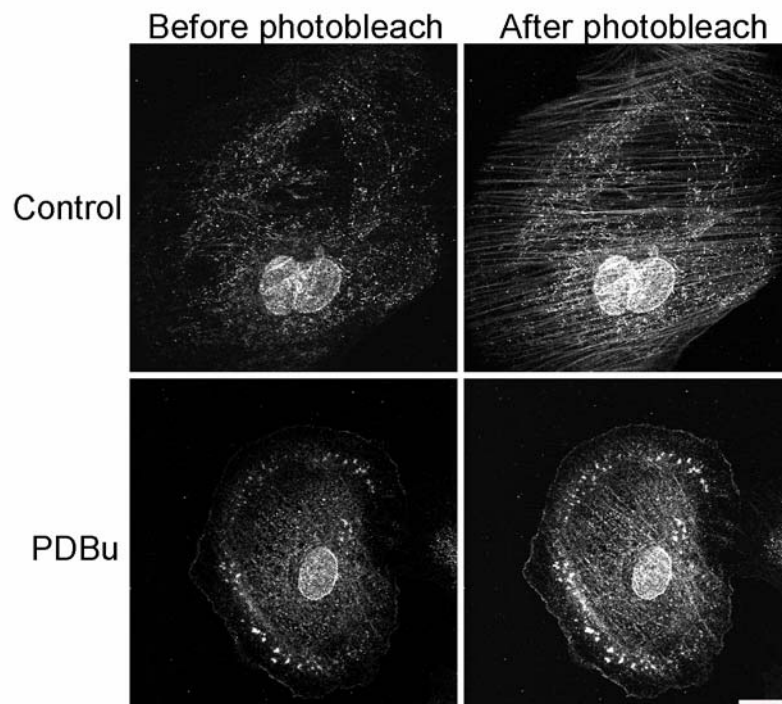


Figure 6.

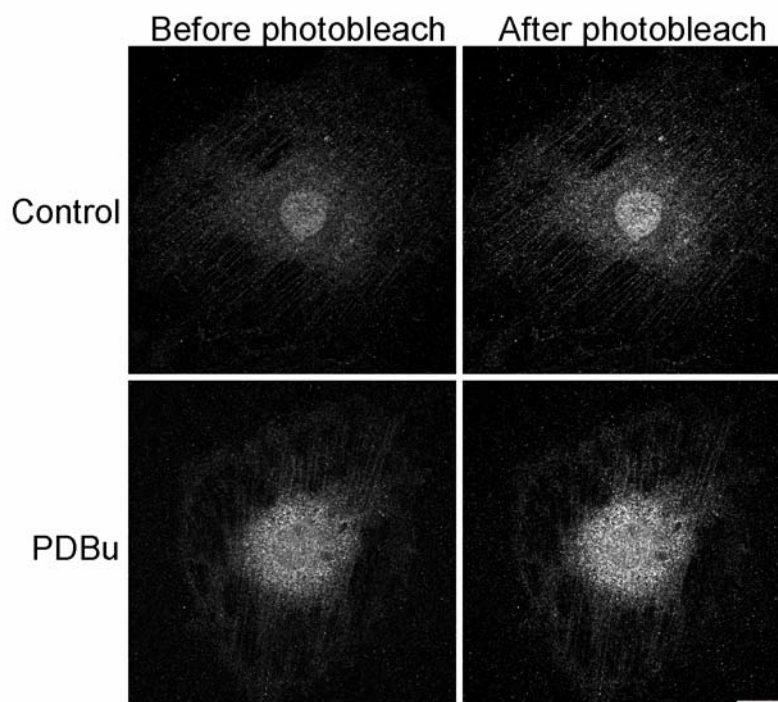


Figure 7.

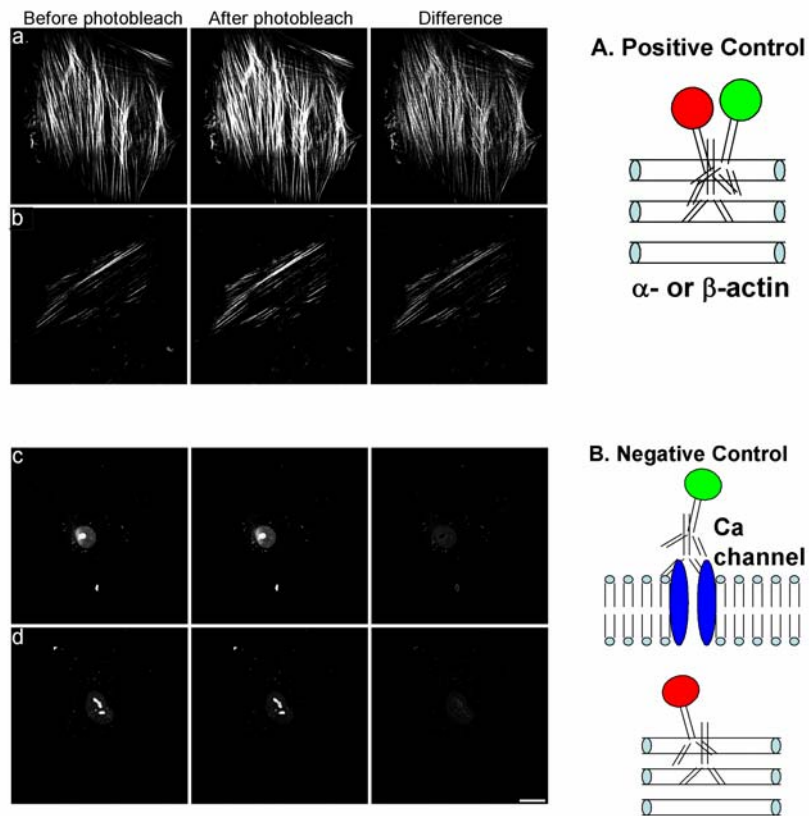


Figure 8.

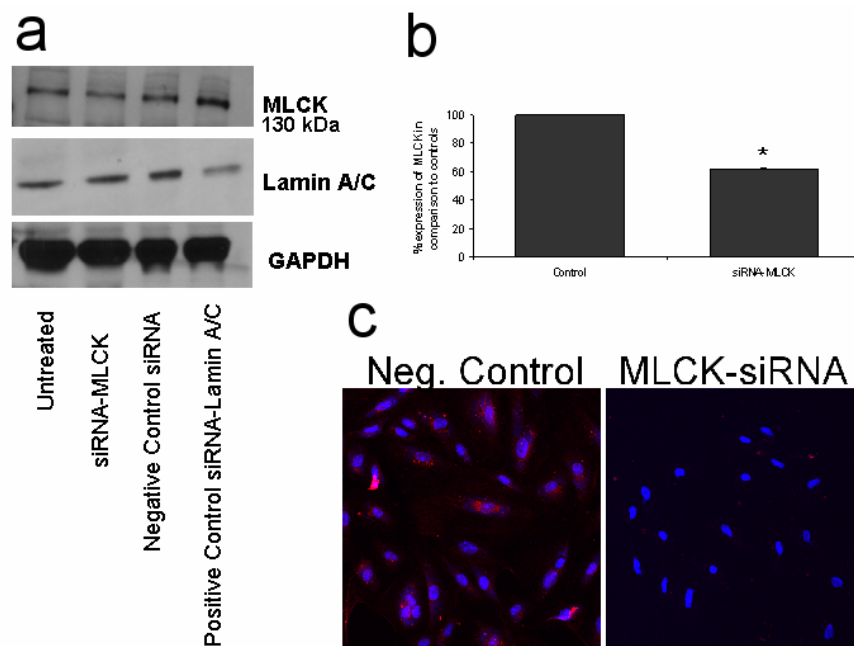


Figure 9.

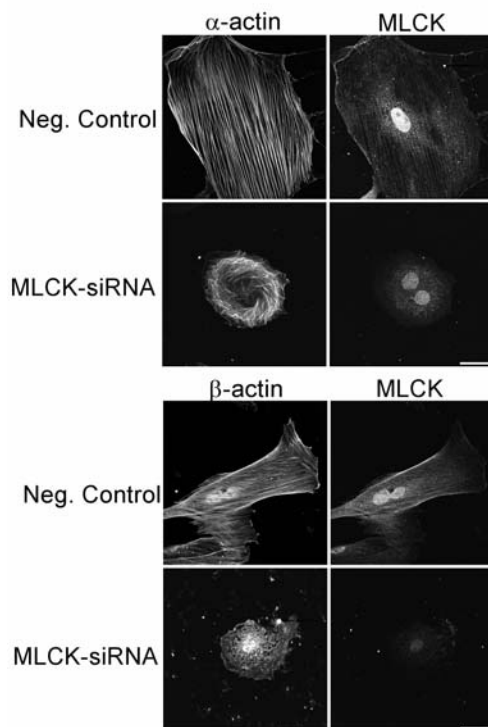


Figure 10.

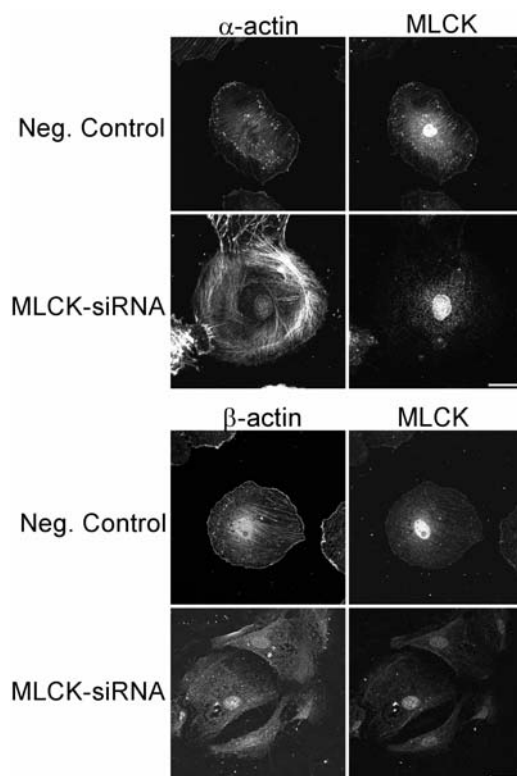


Figure 11.

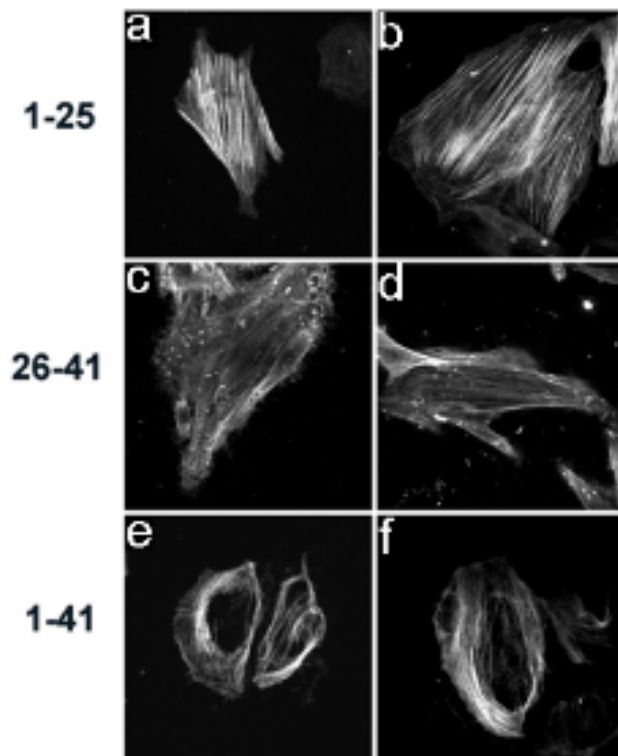


Figure 12.

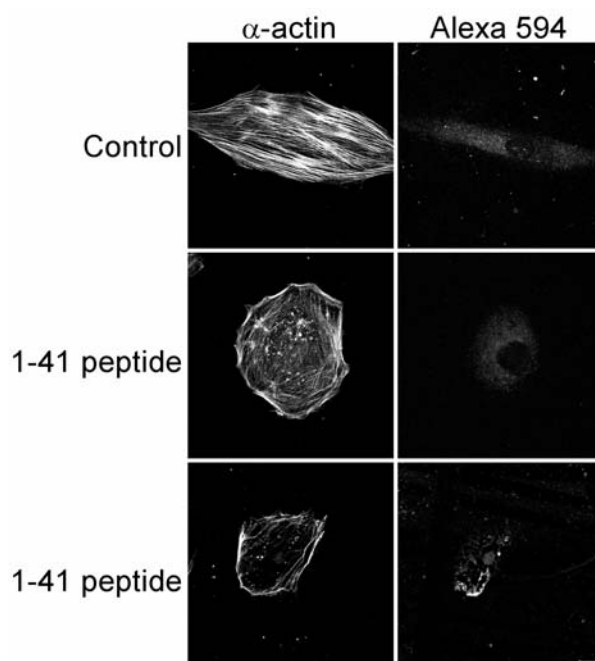


Figure 13.

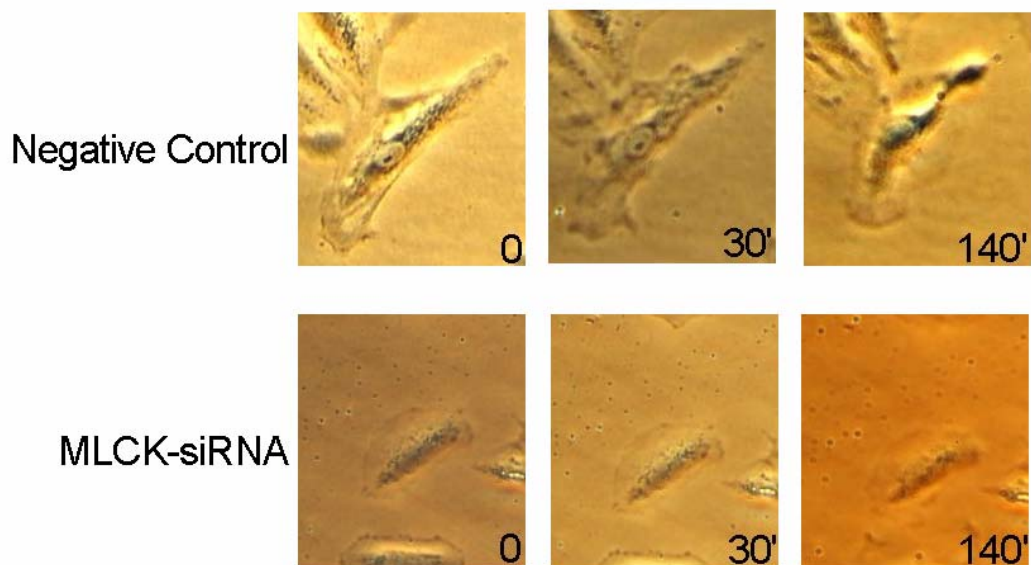


Figure 14.

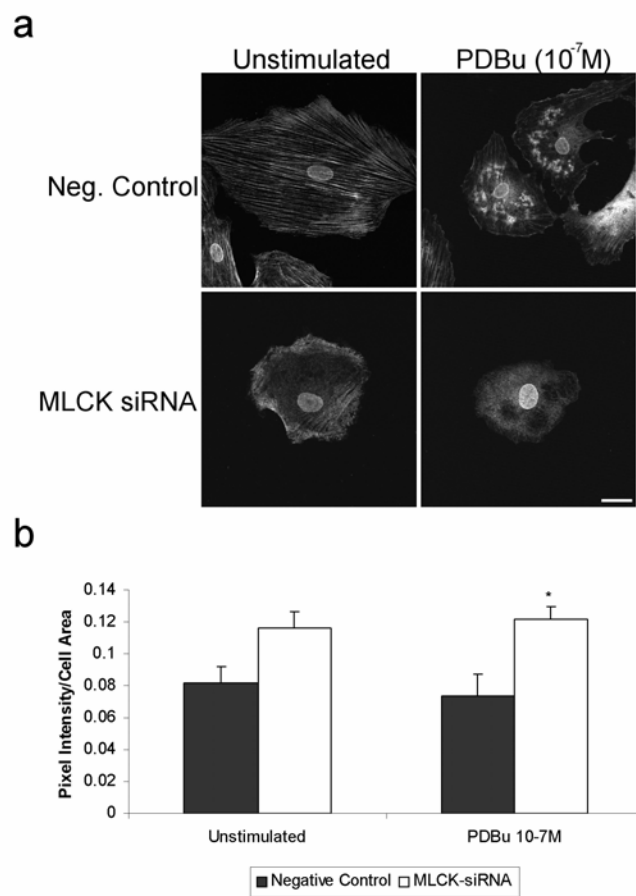


Figure 15.

Chapter Three

MLCK/Actin Interaction in Contracting Rat Aortic Tissue

Thatcher¹ S.E., J.E. Black¹, H. Tanaka², and G.L. Wright¹.

¹Department of Pharmacology, Physiology, and Toxicology, The Joan C. Edwards School of Medicine, Marshall University, Huntington, WV 25704.

²Department of Molecular and Cellular Pharmacology, Gunma University, Maebashi, Japan

Correspondence to:

Gary L. Wright
Professor of Pharmacology, Physiology, and Toxicology
The Joan C. Edwards School of Medicine
Marshall University
Huntington, WV 25704 USA
Phone: 304 696 7368
Fax: 304 696 7381
E-mail: wrightg@marshall.edu

Running title: MLCK/Actin interaction in contracting tissue

Abstract

Myosin light chain kinase (MLCK) is a multifunctional protein with the ability to bind to actin stress filaments at its N-terminus. However, it is unknown how the protein-protein interaction occurs in contracting rat aorta. Therefore, we used confocal microscopy and fluorescent resonance energy transfer (FRET) to better understand the interaction of MLCK with actin stress filaments during phorbol 12, 13-dibutyrate (PDBu)-induced contractions. MLCK/ α -actin did show a significant increase in interaction after 10 minutes of stimulation with PDBu. This interaction decreased midway through contraction and returned to baseline once plateau of contraction had occurred. The MLCK/ β -actin interaction was unchanged at each point of contraction except during the plateau in force generation. This data was supported with co-immunoprecipitations suggesting that MLCK interacts differently with the two predominant isoforms of actin in rat aorta during contraction and remodeling of the cytoskeleton.

Keywords: FRET, phorbol, remodeling, cytoskeleton

Introduction

Myosin light chain kinase (MLCK) is a serine/threonine protein kinase which phosphorylates the regulatory light chain (RLC) of myosin at the serine-19 site (Kamm and Stull, 1985). Recently, it has been established that MLCK binds to actin filaments via its N-terminus with an amino acid motif (DVRXXL) and bundles actin filaments in vitro (Gao et al., 2001). Bundling of actin is abolished upon activation of the calcium-calmodulin ($\text{Ca}^{2+}/\text{CaM}$) complex; however, certain contractile agonists activate smooth muscle tissue without a concomitant increase in calcium or RLC phosphorylation (Deng et al., 2001, Fukuzaki et al., 1992, Miura et al., 1997, Oishi et al., 1991). One contractile agonist that falls into this category is phorbol 12,13-dibutyrate (PDBu). PDBu, a tumor promoter, activates protein kinase C- α (PKC- α) which activates C protein inhibitor-17kDa (CPI-17) and causes inhibition of myosin light chain phosphatase (Vorotnikov et al., 2002). Earlier studies have shown PKC- α translocation to the plasma membrane and actin remodeling to structures referred to as podosomes in the A7r5 smooth muscle cell line under PDBu stimulation (Fultz et al., 2000, Li et al., 2001a). MLCK is also localized to the podosome and shows increases in α -actin interaction; however, β -actin did not show any increase in interaction (unpublished observations). siRNA studies have shown that MLCK is needed in the formation of podosomes (unpublished observations). Other proteins which also bind to actin filaments (calponin and caldesmon) have been shown to be important for the development of podosomes in A7r5 cells (Eves et al., 2006, Gimona et al., 2003). However, it is not known if information from cultured cells can be applied to smooth muscle cells in aortic tissue. Therefore, these studies were performed to

provide information about the PDBu-induced contraction and the nature of protein-protein interaction between MLCK and α - β -actin in the rat aorta.

Materials & Methods

Chemicals. Unless otherwise stated all reagents were purchased from Sigma (St. Louis, MO).

Immunohistochemistry. Rat aortae were hung and contracted as described previously (Wright and Hurn, 1994). Aortae were removed and cut along the long face of the vessel (longitudinal cut) as well as kept intact and cut in cross-section. No differences in protein-protein interaction were observed between the different sections and therefore data were pooled. After contraction with PDBu for 10, 20 minutes or until contraction reached plateau, the tissues were spread on aluminium foil and snap frozen in liquid nitrogen. Tissue was then kept in a -70°C freezer until sectioning could be performed. Tissue sections were cut on an IEC cryotome in 8 micron sections and placed on poly-L-lysine coated slides. Sections were fixed and permeabilized by ice-cold acetone for 1 minute and rinsed three times in PBS/0.5% Tween-20 (PBS-T), pH 7.5. Tissue was then pre-blocked with 5% nonfat milk and rinsed with PBS-T before applying the first primary antibody at a concentration of 1:500 overnight at 4°C (MLCK, K36 clone). The secondary antibody, Alexa 488 IgG (Molecular Probes, Eugene, OR), was applied at a concentration of 1:250 for 1 hour in PBS. The tissue sections were pre-blocked again to remove excess secondary antibody and rinsed with PBS/0.5% Tween-20. Actin or myosin was then probed (α -actin, clone 1A4) (β -actin, clone AC-15) (myosin, clone C5C.S2, Covance) at a concentration of 1:500 for 1 hour. Alexa 568 IgG (for actin) or Alexa 546 IgM (for myosin) was applied at a concentration of 1:250 for 1 hour. Cell nuclei were stained with TO-PRO-3 (Molecular Probes) at a 1:250 concentration for 1 hour. Tissues were rinsed, placed in Gelmount (Biomedica Inc, Foster City, CA) and coverslips applied (24 x 50mm, thickness 1, Fisher Inc., Chicago, IL). Positive and

negative controls were treated in the same manner, however positive controls had both fluorophores (Alexa 488 and Alexa 568) used to target the single primary antibody. In the negative controls, cholera toxin subunit-B was used to probe the lipid bilayer (Alexa 488 conjugate 20 $\mu\text{g}/\text{mL}$, Molecular Probes, Eugene OR) and actin was then probed with an Alexa 568 fluor. No colocalization was seen with the negative controls.

Confocal/FRET Microscopy. Immunostained tissues were mounted on a Nikon Diaphot microscope and confocal microscopy was performed with a BioRad Model 1024 scanning system equipped with a krypton/argon laser. For FRET analysis, MLCK was labeled with Alexa 488 and served as the donor component of the system. α -Actin, β -actin, and myosin were labeled with Alexa 568 or Alexa 546 and served as the acceptor molecules. The donor molecule (MLCK) was directly excited and the resulting emission was obtained with a 522DF32 bandpass filter. However, a portion of the energy of emission was transferred to neighboring Alexa 568 fluorophore resulting in emission that was captured on a second channel with a HQ598/40 bandpass filter. Subsequently, the sample was excited at the 568 nm laser line at 100% power to photobleach the acceptor (α -actin, β -actin) molecule and a second image of the cell was acquired again at the 488 nm laser line with the multichannel set to obtain MLCK fluorescence (522DF32) and to verify the absence of acceptor label 568 emission (HQ598/40). An intensity profile was generated for each image (Image J Software, NIH) and the resulting plot was analyzed with Peakfit V4.11 software (SPSS Science, Richmond, CA) to obtain the area under the curve. The values were then used to calculate the increase in fluorescence intensity after photobleaching. Because resonance energy transfer can only occur if the donor and

acceptor molecules are sufficiently close to one another; the resulting values were analyzed in comparison of treated and control cells as an index of % increase in donor fluorescence for MLCK or examined as % of control (Table 6).

Tissue Co-immunoprecipitations. Rat aortae were homogenized (7-9 aortic rings for each treatment) using a Con-Torque Power Unit (Eberbach Corp., Ann Harbor, MI) in 1.5 mLs of lysis buffer (10 mM MOPS, 1% NP-40, 5 mM EDTA, 0.5 mM EGTA, 1 mM DTT, 50 mM MgCl₂, 300 mM NaCl, 1 mM PMSF, 50 µg/mL leupeptin, chymostatin, and pepstatin A) for a period of 2-3 minutes and placed on ice. Tissue lysate was then sonicated for 10 seconds on a high setting and centrifuged at 14,000 rpm for a period of 5 minutes to clear solution of cellular debris. Supernatant was kept at -70°C until BCA analysis (Pierce, Rockford, IL) could be performed. Protein concentration was determined and equal amounts of sample were loaded onto Protein A/G beads (Pierce, Rockford, IL) conjugated to anti-MLCK antibodies (clone K36) in Immunopure A Binding Buffer (Pierce) overnight at 4°C. Samples were centrifuged (1000 g) for 1 min and rinsed with PBS/0.02% sodium azide six times to rid sample of non-specific protein. Samples were treated with 2X SDS-sample buffer and boiled for a period of 10 minutes. The supernatant was subjected to 12% SDS-PAGE and probed with either α - or β -actin antibodies. PVDF membranes were treated with ECL reagents and scanned using an Epson 2580 photo scanner. Autoradiograms were evaluated using Image J software.

Statistics. All experiments were performed in triplicate unless otherwise indicated. Differences between treatment groups were evaluated by Student's t-test and one-way

ANOVA using Sigma Stat V.2.03 (SPSS Science Inc., San Rafael, CA). Differences were considered significant at $p < 0.05$. Results are presented as means \pm SEM.

Results

Protein-protein interaction has been studied extensively using yeast two-hybrid systems; however, FRET allows for the quantitative measurement of protein interaction in the cell's natural environment. This proves to be advantageous when studying cells under contractile stimulation. In order to calibrate our FRET system, we used positive and negative controls to find our maximum and minimum FRET response (Figure 16). Our positive control values were higher than our maximum experimental values for MLCK and actin (% increase in donor fluorescence, positive control α -actin 249.7 ± 12.2 versus MLCK/ α -actin 10 minute stimulation, 207.8 ± 13.9 ; positive control β -actin 221.4 ± 9.1 versus MLCK/ β -actin zero timepoint 153.1 ± 3.5). This held true for myosin as well (positive control myosin, 188 ± 9.1 versus MLCK/myosin zero timepoint 102.4 ± 8.3). The cholera toxin subunit-B (CT-B) was utilized to label lipid in the membranes of smooth muscle cells and was not shown to colocalize with either actin or myosin inside of the cell (data not shown).

In order to gain perspective into cell orientation and size, cell nuclei were labeled in our samples. It was found that MLCK and α -actin had high levels of colocalization ten minutes into the PDBu contraction (Figure 17A). We also obtained samples twenty minutes after the zero timepoint as well as during the plateau phase of smooth muscle contraction (Figure 17B). MLCK/ α -actin interaction increased during the 10 minute stimulation and fell back to control levels during 20 minutes and plateau (Table 6).

These data were in agreement with colocalization micrographs and co-immunoprecipitations (Figure 17, 19). The MLCK/ α -actin interaction that was evident in

co-immunoprecipitations was compared to the input of actin (tissue lysate) that was placed in the system. The trend was again seen during the 10 minute stimulation (Table 7). It is interesting to note that MLCK interacts with only a small portion of the entire actin pool; however, it has been noted in other studies that this interaction is important in cytoskeletal remodeling and contraction of the smooth muscle cells (Bao et al., 2002, Kishi et al., 2000).

Evaluation of the MLCK/ β -actin interaction was strikingly different. FRET values indicated that MLCK/ β -actin interaction did not change significantly until plateau was achieved (Table 6). When these data were compared to co-immunoprecipitations, the studies did not show a dramatic change in endpoint data when compared to controls (Figure 19B). It was evident that when the MLCK/ β -actin interaction was compared to the input of actin into the system, the amount of MLCK that was associated with β -actin was less than the MLCK and α -actin interaction (Table 7 and Figure 19A). This also correlated with the FRET values obtained in zero timepoint tissues (MLCK/ α -actin 179.6 ± 17.2 ; MLCK/ β -actin 153.1 ± 3.5 , % of increase in donor fluorescence).

Our plans will be to study other actin-binding proteins (e.g. calponin and caldesmon) to see how these interactions occur with actin as well. FRET and co-immunoprecipitations for MLCK/myosin did not show interaction therefore it was not included in the present data set. Collectively, the data suggest that MLCK interaction with actin isoforms differs depending on the isoform studied and may be important in understanding contractile mechanisms of smooth muscle. Finally, observation of cells in the rat aorta indicated that

MLCK and α -actin interact at discrete microdomains in the periphery of the cell (Figure 19). A7r5 cells also show MLCK/ α -actin interaction in adhesive structures in the periphery of the cell referred to as podosomes. However, it remains to be determined if vascular smooth muscle cells contained within an extracellular matrix act in a similar fashion to those during contraction in cell culture.

Discussion

Smooth muscle contraction has been studied extensively, but only recently have improvements in imaging allowed for better measurement of protein-protein interaction. FRET gives the ability to measure interaction within the cell and monitor differences upon contractile stimulation (Isotani et al., 2004). Here we looked at two different isoforms of actin and myosin II to better understand their interaction with MLCK. In vitro data has shown that MLCK has a high affinity actin-binding site located within the N-terminus of the molecule (Hayakawa et al., 1999b). Upon activation of the Ca²⁺/CaM complex, the ability to bundle actin is destroyed thus allowing myosin II to cycle along the thin filament. PDBu, on the other hand, does not induce a high calcium response and the contraction is extremely slow in contrast to high calcium agonists such as A23187 or potassium depolarization (Li et al., 2001b). MLC phosphorylation also undergoes only a slight increase in the initial stages of PDBu contraction and it is thought that other kinases play a role in the calcium independent contraction (e.g. Rho-kinase and Integrin-linked kinase)(Chrzanowska-Wodnicka and Burridge, 1996, Deng et al., 2001, Miura et al., 1997). Therefore, the ability for MLCK to bundle actin should remain intact during the PDBu-induced contraction. FRET and co-immunoprecipitations indicated this with MLCK showing enhanced and diminished ability to bind to actin during certain aspects of the PDBu contraction. The homology of α - and β -actin is >95%, leaving a 10-12 amino acid residue portion difference in the N-terminus of the two proteins. Whether MLCK interacts with this specific N-terminal sequence is still not known at this time.

Fultz et al. (2000), have shown that α -actin and β -actin remodel differently in the presence of phorbol esters in the A7r5 smooth muscle cell line. α -Actin typically remodels into adhesive structures called podosomes while the β -actin remains in filamentous form. The tissue data suggest a similar remodeling phenomenon; however, aortic tissue showed a quicker response (within 10 minutes) of the MLCK/ α -actin interaction, whereas the MLCK/ α -actin interaction in A7r5 cells showed enhancement of interaction after a 30-minute stimulation (unpublished observations). The reason for the time difference is unclear, but the data suggest recruitment of MLCK to the α -actin filaments during the PDBu-induced contraction.

The MLCK/ β -actin interaction remained unchanged during the development of tension in rat aorta, perhaps indicating its role as a structural scaffold allowing the α -actin to remodel with MLCK into microdomains in the periphery of the cell. Despite the conflicting data for the plateau phase of contraction, it has been shown that MLCK binds to both α -actin and β -actin filaments. When comparisons were made on the amounts of α -actin that interacts with MLCK, a 12-20% interaction was discovered with the high range occurring during the 10-minute stimulation. The interaction between MLCK and β -actin showed a 3-8% range and these values decreased as plateau was achieved. Although these results could be due to differences in antibody affinity, it is interesting to note that α -actin and β -actin ratios have been found in similar proportions in other studies (Otey et al., 1987, Otey et al., 1988).

MLCK and its ability to bind to myosin II at its C-terminus has been documented, but the affinity is rather weak in comparison to actin (Stull et al., 1998). Although we noted a FRET response in our positive controls for myosin, we could not see a significant increase in FRET or interaction via co-immunoprecipitations for the MLCK/myosin interaction. Reasons for this could be that the MLCK/myosin interaction is transient or was abolished due to immunohistochemical/co-immunoprecipitation protocols. Another could be that direct MLCK/myosin interaction is not needed for the PDBu-induced contraction.

Taken together, the data suggest that MLCK interacts differently with α - and β -actin acts during PDBu-induced contraction. This difference supports earlier studies in actin isoform-specific remodeling in the A7r5 smooth muscle cell line.

References

- Bao J, K Oishi, T Yamada, L Liu, A Nakamura, MK Uchida, and K Kohama (2002). Role of the short isoform of myosin light chain kinase in the contraction of cultured smooth muscle cells as examined by its down-regulation. *PNAS* **99**(14): 9556-9561.
- Battistella-Patterson AS, ME Fultz, C Li, W Geng, M Norton, and GL Wright (2000). PKC α translocation is microtubule-dependent in passaged smooth muscle cells. *Acta. Physiol. Scand.* **170**: 87-97.
- Chrzanowska-Wodnicka M, and K Burridge (1996). Rho-stimulated contractility drives the formation of stress fibers and focal adhesions. *J. Cell. Bio.* **133**(6): 1403-1415.
- Deng JT, JE Van Lierop, C Sutherland, and MP Walsh (2001). Ca²⁺-independent smooth muscle contraction (a novel function for integrin-linked kinase). *J. Biol. Chem.* **276**(19): 16365-16373.
- Dykes AC, ME Fultz, ML Norton, and GL Wright (2003). Microtubule-dependent PKC- α localization in A7r5 smooth muscle cells. *Am. J. Physiol. (Cell Physiol.)* **285**: C76-C87.
- Eves R, Webb BA, Zhou S, and Mak AS (2006). Caldesmon is an integral component of podosomes in smooth muscle cells. *J. Cell. Sci.* **119**: 1691-1702.
- Fukuzaki A, O Suga, H Karibe, Y. Miyauchi, T Gokita, and MK Uchida (1992). Ca²⁺-independent contraction of uterine smooth muscle induced by vanadate and its inhibition by Ca²⁺. *Eur. J. Pharmacol.* **220**: 99-102.
- Fultz ME, C Li, W Geng, and GL Wright (2000). Remodeling of the actin cytoskeleton in the contracting A7r5 smooth muscle cell. *J. Muscle Res. & Cell Motil.* **21**: 775-787.
- Gao Y, Ye L, Kishi H, Okagaki T, Samizo K, Nakamura A, Kohama K (2001). Myosin light chain kinase as a multifunctional regulatory protein of smooth muscle contraction. *IUBMB Life* **51**: 337-344.
- Gimona M, Kaverina I, Resch GP, Vignal E, and Burgstaller G (2003). Calponin repeats regulate actin filament stability and formation of podosomes in smooth muscle cells. *Mole. Biol. Cell* **14**: 2482-2491.
- Hayakawa K, T Okagaki, L Ye, K. Samizo, S Higashi-Fujime, T Takagi, and K Kohama (1999). Characterization of the myosin light chain kinase from smooth muscle as an actin-binding protein that assembles actin filaments in vitro. *Biochimica et Biophysica Acta* **1450**: 12-24.
- Isotani E, Zhi G, Lau KS, Huang J, Mizuno Y, Persechini A, Geguchadze R, Kamm KE, and Stull JT (2004). Real-time evaluation of myosin light chain kinase activation in

smooth muscle tissues from a transgenic calmodulin-biosensor mouse. *Proc. Natl. Acad. Sci.* **101**(16): 6279-6284.

Kamm KE, and Stull JT (1985). The function of myosin and myosin light chain kinase phosphorylation in smooth muscle. *Ann. Rev. Pharmacol. Toxicol.* **25**: 593-620.

Kishi H, T Mikawa, M Seto, Y Sasaki, T Kanayasu-Toyoda, T Yamaguchi, M Imamura, M Ito, H Karaki, J Bao, A Nakamura, R Ishikawa, and K Kohama (2000). Stable transfectants of smooth muscle cell line lacking the expression of myosin light chain kinase and their characterization with respect to the actomyosin system. *J. Biol. Chem.* **275**(2): 1414-1420.

Li C, ME Fultz, J Parkash, WB Rhoten, and GL Wright (2001). Ca²⁺-dependent actin remodeling in the contracting A7r5 cell. *J. Muscle Res. & Cell Motil.* **22**: 521-534.

Miura M, T Iwanaga, KM Ito, M Seto, Y Sasaki, and K Ito (1997). The role of myosin light chain kinase-dependent phosphorylation of myosin light chain in phorbol ester-induced contraction of rabbit aorta. *Pflugers Arch-Eur. J. Physiol.* **434**: 685-693.

Oishi K, H Takano-Ohmuro, N Minakawa-Matsuo, O Suga, H Karibe, K Kohama, and MK Uchida (1991). Oxytocin contracts rat uterine smooth muscle in Ca²⁺-free medium without any phosphorylation of myosin light chain. *Biochem. & Biophys. Res. Comm.* **176**(1): 122-128.

Otey CA, MH Kalnoski, and JC Bulinski (1987). Identification and quantification of actin isoforms in vertebrate cells and tissues. *J. Cell. Biochem.* **34**: 113-124.

Otey CA, MH Kalnoski, and JC Bulinski (1988). Immunolocalization of muscle and nonmuscle isoforms of actin in myogenic cells and adult skeletal muscle. *Cell Motil. & Cytoskel.* **9**: 337-348.

Stull JT, PJ Lin, JK Krueger, J Trewhella, and G Zhi (1998). Myosin light chain kinase: functional domains and structural motifs. *Acta. Physiol. Scand.* **164**: 471-482.

Vorotnikov AV, MA Krymsky, and VP Shirinsky (2002). Signal transduction and protein phosphorylation in smooth muscle contraction. *Biochemistry (Moscow)* **67**(12): 1309-1328.

Figure Legends

Figure 16. A.) Immunohistochemical staining of rat aortae for α -/ β -actin, myosin, and cholera toxin subunit-B (CT-B) “before photobleaching of acceptor” and “after photobleaching of acceptor.” B.) Percent increase in donor fluorescence for positive and negative controls. Positive controls were one primary antibody targeted with two fluorophores (Alexa 488 and Alexa 568). Negative controls were CT-B targeted with the acceptor being either α - or β -actin. No colocalization was evident with negative controls. Actin and myosin micrographs are in cross-section. CT-B micrograph is in longitudinal-section. The white bar represents 20 μ m.

Figure 17. A.) Triple staining of MLCK (green), α -actin (red), and nuclei (blue) in longitudinal cut of rat aorta from control (unstimulated) and 10 minute exposure to PDBu (10^{-7} M). Color figure legend is found under “contracted” confocal image. Yellow represents colocalization of MLCK and α -actin. Magenta represents colocalization of α -actin and cell nuclei. White arrows represents the direction in which the cells are oriented. Note the decrease in cell length in the contracted aortic cells. The white bar represents 20 μ m. B.) Tissue was evaluated at time zero (A), 10 minutes after exposure to PDBu (B, start), 20 minutes after exposure to PDBu (C, midpoint) and at endpoint of contraction (D, plateau).

Figure 18. Increased magnification of rat aorta depicting a single cell. Triple staining of MLCK (green), α -actin (red), and nuclei (blue) in longitudinal cut of rat aorta. Color figure legend is found under “merge” confocal image. Note the colocalization between

α -actin and MLCK at discrete microdomains in the periphery of the cell. Micrograph labeled “Difference” is the image subtraction of the “Before photobleach” image and the “After photobleach” image. Note the areas of colocalization indicate a positive FRET value. Scale bar represents 5 μ m.

Figure 19. A.) Immunoblots of MLCK co-immunoprecipitations probed for α - and β -actin. “TL” represents tissue lysate or input into the system with “C” representing (control), “10” (10 minutes after PDBu), “20” (20 minutes after PDBu), and “End” (endpoint of contraction). B.) Line graph analysis of treatment groups based on percent of control. Asterisk represents a significant difference between control and treatment with $p < 0.05$.

Table 6. FRET analysis of MLCK/Actin interaction in rat aorta.

	<u>α-actin/MLCK</u>	<u>β-actin/MLCK</u>
Control (zero timepoint)	100 \pm 3.5	100 \pm 2.6
10 min. (start)	117.1 \pm 4.1*	95.1 \pm 1.7
20 min. (midpoint)	91.1 \pm 2.2	97.0 \pm 2.5
Endpoint (plateau)	95.1 \pm 2.3	72.6 \pm 0.9*

Data are presented as percent of control with values summarized as means \pm SEM. Asterisks represent a significant difference between control and treatment group with $p < 0.05$.

Table 7. Percent of MLCK and α -/ β -actin interaction in comparison to tissue lysate.

	<u>α-actin/MLCK</u>	<u>β-actin/MLCK</u>
Control	11.3 \pm 2.9	5.8 \pm 2.6
10 min.	16.9 \pm 5.9	5.5 \pm 2.3
20 min.	11.8 \pm 5.1	3.9 \pm 1.6
Endpoint	12.0 \pm 4.3	3.4 \pm 1.4

Data are presented as means \pm SEM.

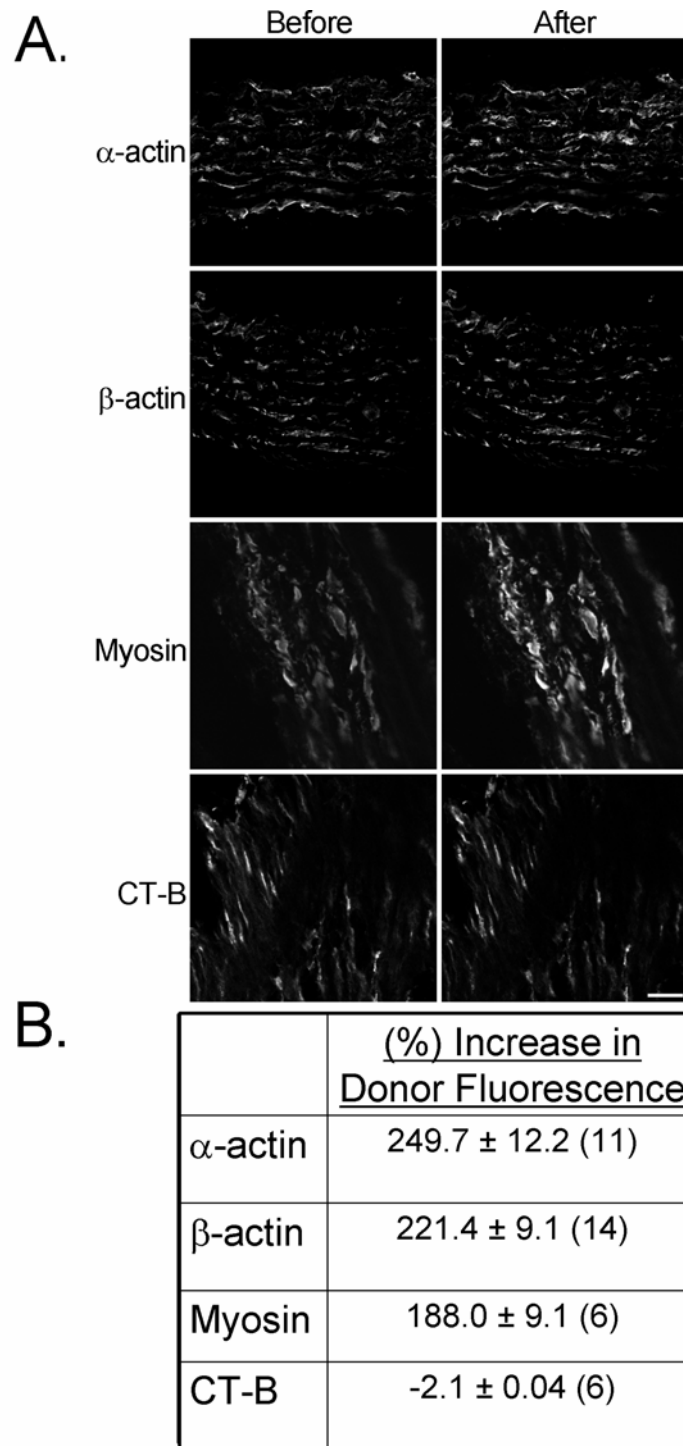


Figure 16.

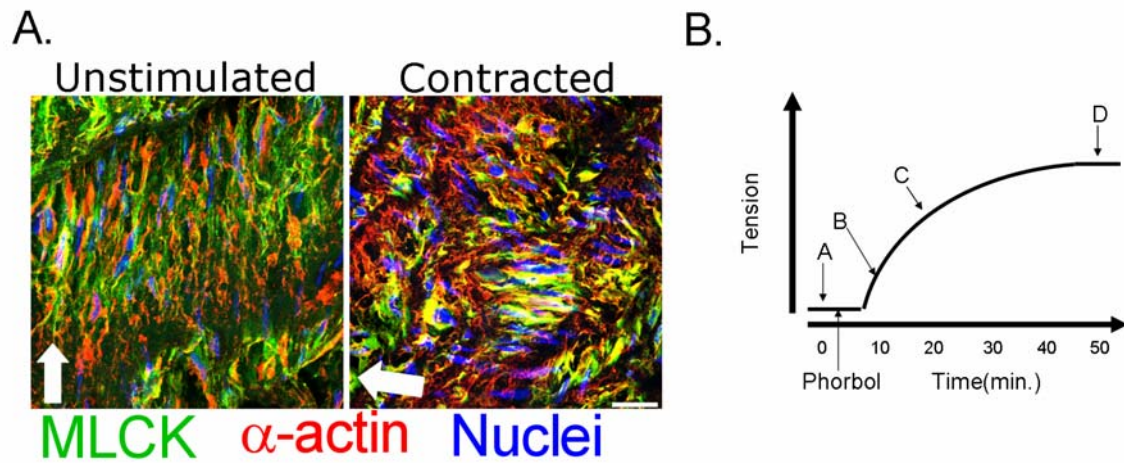


Figure 17.

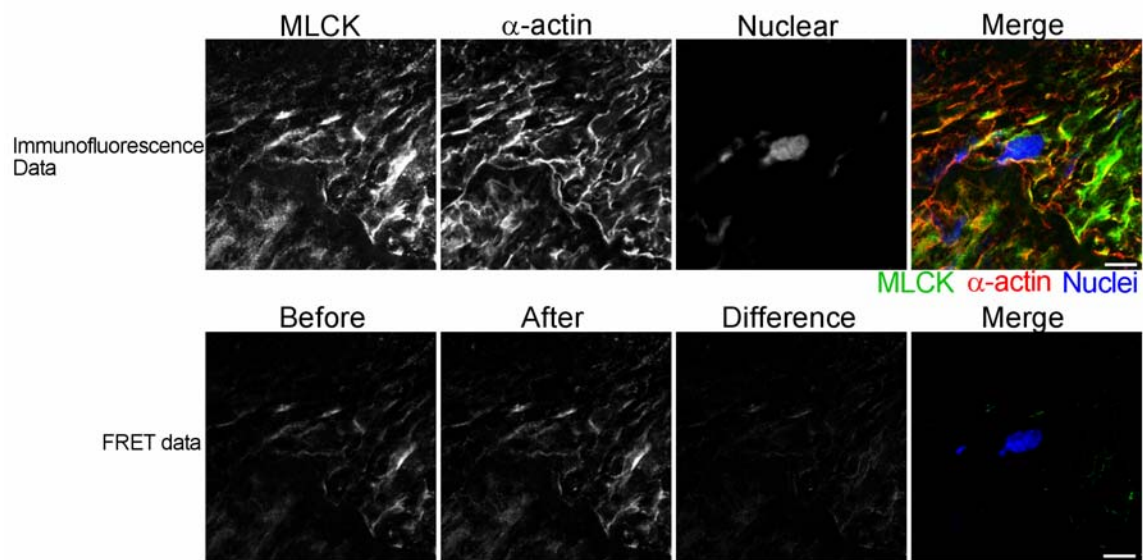


Figure 18.

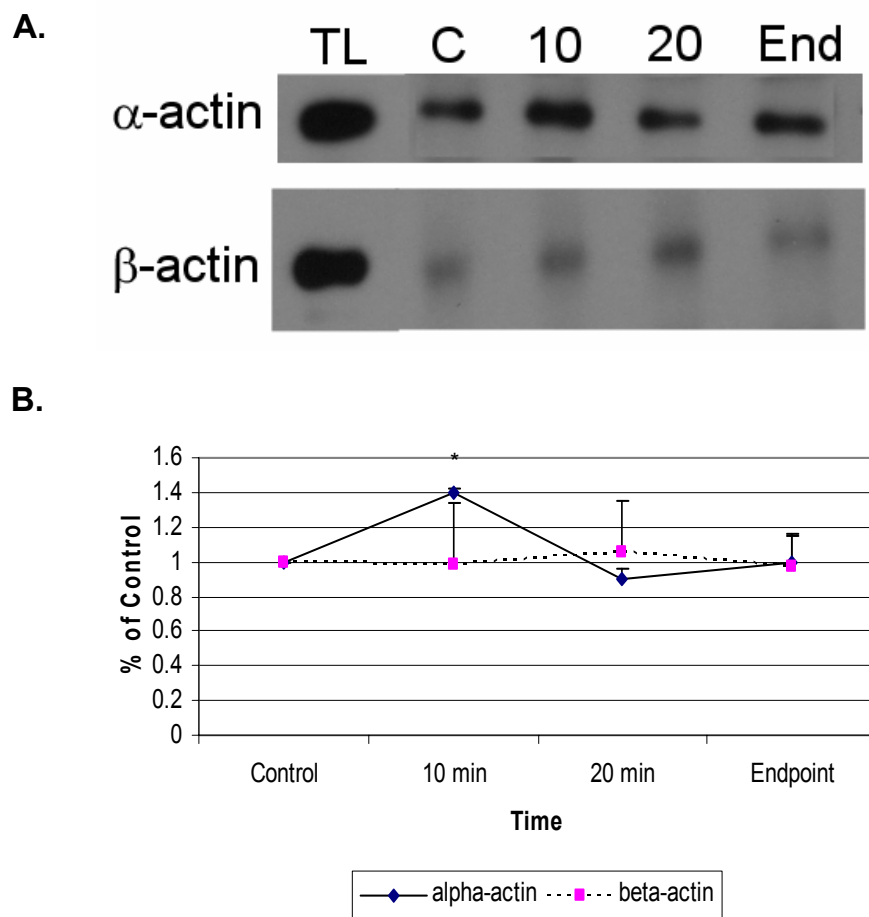


Figure 19.

Chapter Four

Summary and Conclusions General Discussion

Here we examined the role of MLCK and its binding to α - and β -actin in the A7r5 cell and rat aorta. MLCK did show significant binding to α -actin and was located in the podosome of the A7r5 cell. RNAi assays revealed that MLCK was necessary for podosome formation and filament stabilization. Despite MLCK downregulation, RLC phosphorylation was not affected by the siRNA indicating that the kinase domain of MLCK was not influential in podosome development or filament stabilization. This is the first study to link the N-terminus of MLCK as a necessary component in the formation of podosomes and binding to both α - and β -actin.

MLCK also shows interaction with both α - and β -actin in rat aortae. FRET analysis and co-immunoprecipitations confirm differential binding during the time course of the PDBu-induced contraction. These studies suggest that MLCK may be recruited to actin filaments and this may contribute to force development and tension maintenance in vascular smooth muscle.

In Figure 20, a model is proposed to help explain how the MLCK/ α -actin interaction takes place and disengagement of MLCK to the α -actin filament in the presence of Ca^{2+} /CaM. The diagram suggests that actin and myosin are kept in register with one another through MLCK binding and that MLCK will allow for power stroke along one α -actin filament while remaining bound to the other β -actin filament. This model could explain why α -actin remodels into podosomes while β -actin remains in filamentous form in the PDBu-induced contraction.

In the resting configuration prior to the initiation of contraction (Figure 20A), MLCK would act to cross-link actin filaments, stabilizing the contractile cytoskeleton in a “pseudo-sarcomere” with actin filaments in register with myosin filaments. In the presence of Ca^{2+} /CaM (Figure 20B) concurrent with the activation of MLCK kinase activity, the loss of binding at the Ca^{2+} /CaM-sensitive site would serve to destabilize actin filament arrangement allowing filament sliding and freeing actin filaments for reorganization during cell shortening.

The results suggest that α -actin is more susceptible to MLCK/ Ca^{2+} -CaM destabilization indicating future studies to investigate the dynamics of MLCK binding with α - and β -actin filaments. In combination with the present findings, the model further predicts that PKC-mediated events may contribute significantly to α -actin remodeling during contraction and could involve modulation of MLCK cross-linking activity.

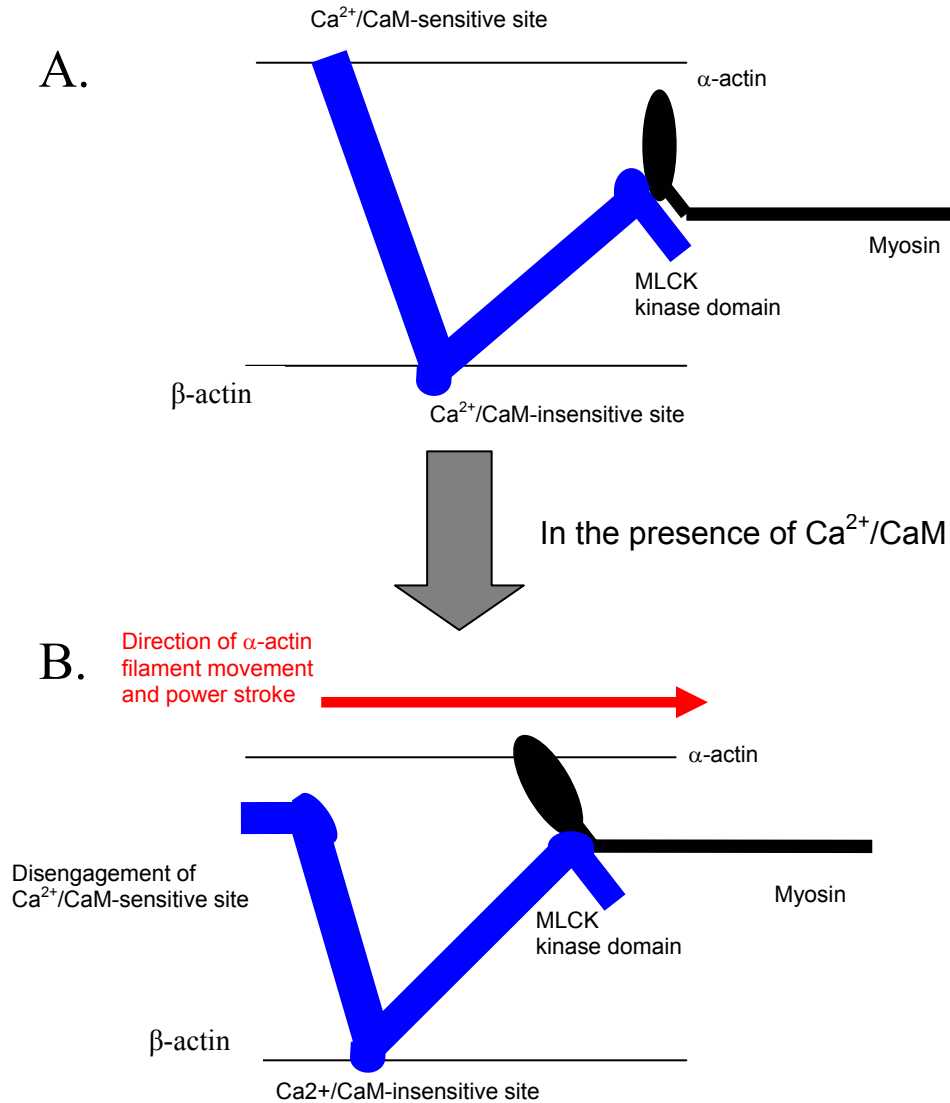


Figure 20. Proposed model for the MLCK/actin interaction in vascular smooth muscle. Note that in the absence of Ca²⁺/CaM (A), the Ca²⁺/CaM-sensitive and –insensitive sites are bound to two actin filaments. This protein conformation positions the myosin filament and α-actin filament so that there is no interaction. Upon calcium influx and CaM activation (B), MLCK undergoes a conformational change to disengage the Ca²⁺/CaM-sensitive site allowing for myosin and α-actin interaction and subsequent power stroke to occur. Note that while the α-actin filament moves to the right, the β-actin filament is kept in register with the myosin filament.

Future Work

The possibility that podosomes may be similar or identical to invadopodia suggests that smooth muscle has directed cellular motility after breakdown of the ECM. This migration has been documented in cardiovascular problems such as aneurysm and atherosclerosis. Work by the Mak lab, using the explant method, has indicated that vascular smooth muscle cells display podosomes (Webb et al., 2006). It has also been documented that inhibition of MMPs through the antibiotic, doxycycline, decreases the severity and incidence of abdominal aortic aneurysm (AAA) (Manning et al., 2003). It will be of interest to see if the structure and function of podosomes in the A7r5 cell are similar to those in vascular smooth muscle and if inhibition of podosomes will decrease or abolish the severity of cardiovascular diseases.

References

- Manning, M. W., L. A. Cassis and A. Daugherty. 2003. Differential effects of doxycycline, a broad-spectrum matrix metalloproteinase inhibitor, on angiotensin II-induced atherosclerosis and abdominal aortic aneurysms. *Arterioscler Thromb Vasc Biol.* **23**(483-488).
- Webb, B. A., R. Eves and A. S. Mak. 2006. Cortactin regulates podosome formation: roles of the protein interaction domains. *Exp Cell Res.* **312**(760-769).



CURRICULUM VITAE

NAME: Sean Eric Thatcher

ADDRESS: Joan C. Edwards School of Medicine
Marshall University
Department of Physiology, Pharmacology, and Toxicology
1542 Spring Valley Dr.
Huntington, WV 25704 USA

OFFICE PHONE: (304) 696-7363

FAX: (304) 696-7381

E-MAIL: thatcher1@marshall.edu

HOME PHONE: (304) 429-3136

HOME ADDRESS: 1616 Spring Valley Dr. Apt. #19
Huntington, WV 25704, USA

COLLEGE: Ph.D. in Biomedical Science, Marshall University, May 2007
M.S. in Biology, Morehead State University, 2001
B.S. in Biology, Morehead State University, 1999

TEACHING: Graduate Assistant, Morehead State University
Courses taught: Principles of Biology Lab
Course Supervisor: Dr. David Magrane

Graduate Assistant, Morehead State University
Laboratories Prepared: Genetics and Biochemistry
Supervisor: Dr. Craig Tuerk

MEMBER:

American Association for the Advancement of Science

Kentucky Academy of Science

American Society for Cell Biology

American Physiological Society

PUBLICATIONS:

Masters Thesis: Thatcher, S.E. Effects of Butyrate Feeding on Glucose Tissue Metabolism in Exercised Mice. Morehead State University, 2001.

Brown, D., A. Dykes, J. Black, S. Thatcher, M. Fultz, and G.L. Wright. Alpha- and Beta-actin Reorganization in the Contracting A7r5 Smooth Muscle Cell. *Canadian Journal of Physiology and Pharmacology*, In Press.

Sheng, L., H. Tanaka, H. Wang, S. Yoshiyama, H. Kumagai, A. Nakamura, D. Brown, S. Thatcher, G.L. Wright, and K. Kohama. Intracellular signal transduction for migration and actin remodeling in vascular smooth muscle cells following sphingosylphosphorylcholine stimulation. *American Journal of Physiology-Heart and Circulatory Physiology* 291: H1262-H1272, 2006.

PUBLICATIONS IN PROGRESS :

Black, J., A. Dykes, D. Brown, S. Thatcher, and G.L. Wright. FRET Analysis of Actin/myosin Interaction in Contracting Aortic Smooth Muscle. Submitted to *European Journal of Physiology*, August 2006.

Thatcher SE, ME Fultz, H. Tanaka, C. Wright, K. Kohama, and G. Wright. MLCK/actin Interaction in the Contracting A7r5 Smooth Muscle Cell. Submitted to *American Journal of Physiology-Cell Physiology*, August 2006

Thatcher SE, J. Black, H. Tanaka, and GL Wright. MLCK/actin Interaction in Contracting Rat Aortic Tissue. In preparation.

Thatcher SE, JE Black, D Brown, and GL Wright. MMP-2 and MMP-9 Localization in the Contracting A7r5 Smooth Muscle Cell. In preparation.

POSTER PRESENTATIONS:

The Effects of Butyrate Feeding on Glucose Tissue Metabolism in Exercised Mice. Kentucky & Tennessee Academy of Sciences. Murfreesboro, TN. November 2001.

The Influence of Kinase Inhibitors on the Stress Relaxation Response in Rat Aortic Smooth Muscle. Joan C. Edwards School of Medicine Research Day. Huntington, WV. April 2005.

Correlation of force development with α -actin remodeling in smooth muscle: Effects of Specific Kinase Inhibitors. Kentucky Academy of Sciences. Richmond, KY. November 2005.

MLCK/actin Interaction in the Contracting A7r5 Smooth Muscle Cell. ASCB meeting, San Francisco, CA. December 2005.

MLCK/actin Interaction in the Contracting A7r5 Smooth Muscle Cell. Joan C. Edwards School of Medicine Research Day. Huntington, WV. April 2006.

Involvement of MLCK in Actin Stabilization and Podosome Development in the Contracting A7r5 Smooth Muscle Cell. ASCB meeting, San Diego, CA. December 2006.

MMP-2 and -9 Localization in the Contracting A7r5 Smooth Muscle Cell. Joan C. Edwards School of Medicine Research Day. Huntington, WV. April 2007.

MLCK/actin Interaction in Contracting Rat Aortic Smooth Muscle. Experimental Biology, Washington, DC. April 2007.

INVITED PRESENTATIONS:

MLCK/actin Interaction in the Contracting A7r5 Smooth Muscle Cell. Morehead State University, March 14, 2006.

MLCK/actin Interaction in the Contracting A7r5 Smooth Muscle Cell. Wheeling Jesuit College, April 20, 2006.

MLCK/actin Interaction in the Contracting A7r5 Smooth Muscle Cell. Summer Seminar series for WV-INBRE, July 2006.

COMMUNITY SERVICE:

Performed Bio-Rad "Genes in a Bottle" experiment for sixth grade students at Bath County Middle School, Owingsville, KY., May 2006.

Assisted in protein electrophoresis and DNA extraction experiments for Talented and gifted program for Bath County Senior High School, Owingsville, KY., June 2006.

LABORATORY TECHNIQUES:

Cell Culture: Maintenance of passaged rat aortic smooth muscle cells and A7r5 smooth muscle cells

Tissue Extraction: Harvesting of smooth muscle medial layer in rat thoracic aorta, cryotome sectioning of aorta

Contractility: Rat thoracic aorta

Electrophoresis: Polyacrylamide gel electrophoresis (PAGE) for protein analysis, agarose gels for DNA analysis, BCA and Bradford protein assays

Imaging: Confocal Microscopy and related computer software, FRET, wide-field fluorescence microscopy, phase-contrast microscopy, H&E staining

Molecular Biology: Microinjection of A7r5 cells, lipofectamine transfection, electroporation, bacterial transformations, PCR, RT-PCR and DNA extraction and amplification protocols, RNAi

Radiolabels: Radiolabel purification from tissues and measurements using scintillation counters

Animal Surgery: Mice, Rats

LAB VISITS:

Spent 2 ½ months performing experiments in Maebashi, Japan under the supervision of Dr. Kazuhiro Kohama. Techniques learned: myosin light chain phosphorylation assay, collagen fiber assay, and Boyden chamber assay (cell motility assay)

REFERENCES:

Gary L. Wright, Ph.D
Chairman, Department of Physiology
Professor, Department of Physiology
Joan C. Edwards School of Medicine
Marshall University
1542 Spring Valley Dr.
Huntington, WV 25704 USA
(304) 696-7368

William D. McCumbee, Ph.D
Professor, Department of Physiology
Joan C. Edwards School of Medicine
Marshall University
1542 Spring Valley Dr.
Huntington, WV 25704 USA
(304) 696-7366

Elsa I. Mangiarua, Ph.D
Assistant Professor, Department of Physiology
Joan C. Edwards School of Medicine
Marshall University

1542 Spring Valley Dr.
Huntington, WV 25704 USA
(304) 696-6211

David Magrane, Ph.D
Chairman, Department of Biology
Professor, Department of Biology
Morehead State University
103 Lappin Hall
Morehead, KY 40351 USA
(606) 783-2944

Craig Tuerk, Ph.D
Professor, Department of Biology
Morehead State University
103 Lappin Hall
Morehead, KY 40351 USA
(606) 783-2944